# Artemether confers neuroprotection on cerebral ischemic injury through stimulation of the Erk1/2-P90rsk-CREB signaling pathway

Shuai Li [a,1], Tangming Peng [a,c,1], Xia Zhao [a,1], Marta Silva [a], Linlin Liu [a], Wenshu Zhou [a], Ligang Chen [c,**], Wenhua Zheng [a,b,*]

[a] Center of Reproduction, Development & Aging, Faculty of Health Sciences, University of Macau, Taipa, Macau SAR, China and Institute of Translation Medicine, Faculty of Health Sciences, University of Macau, Taipa, Macau SAR, China
[b] Zhuhai UM Science & Technology Research Institute, Zhuhai, China
[c] Department of Neurosurgery, Affiliated Hospital of Southwest Medical University, Luzhou, China

ARTICLE INFO

ABSTRACT

Ischemic stroke is one of the leading causes of death and disability among adults. Despite the economic burden of the disease, available treatment options are still very limited. With the exception of anti-thrombolytics and hypothermia, current therapies fail to reduce neuronal injury, neurological deficits and mortality rates, suggesting that the development of novel and more effective therapies against ischemic stroke is urgent. In the present study, we found that artemether, which has been used in the clinic as an anti-malarial drug, was able to improve the neurological deficits, attenuate the infarction volume and the brain water content in a middle cerebral artery occlusion (MCAO) animal model. Furthermore, artemether treatment significantly suppressed cell apoptosis, stimulated cell proliferation and promoted the phosphorylation of extracellular signal-regulated kinase 1/2 (ERK1/2), P90$^{rsk}$ and cAMP responsive element-binding protein (CREB). Artemether protective effect was attenuated by PD98059, an ERK1/2 inhibitor, administration. Similarly, in oxygen-glucose deprivation/reperfusion (OGD/RP) cell models, artemether pre-treatment induced the suppression of the intracellular ROS, the down-regulation of LDH activity, the reduction of caspase 3 activity and of the apoptosis cell rate and reversed the decrease of mitochondrial membrane potential. As with MCAO animal model, artemether promoted the activation of Erk1/2-P90$^{rsk}$-CREB signaling pathway. This effect was blocked by the inhibition or knockdown of ERK1/2. The present study provides evidences of the neuroprotective effect of artemether unravelling its potential as a new therapeutic candidate for the prevention and treatment of stroke.

## 1. Introduction

Ischemic stroke is one of the leading causes of adult morbidity and mortality worldwide [1]. In China alone, the incidence rate among residents aged 40–74 years has increased by an average of 8.3% per year [2]. By 2030, ischemic stroke-related costs are expected to reach 240.67 billion dollars and still the available therapeutic options are very limited [3]. An ischemic stroke is characterized by the reduction of the cerebral blood flow by thromboembolic occlusion, accounting for about 80% of all types of stroke. Currently, the recombinant tissue plasminogen activator (rtPA) is the only FDA-approved drug for the treatment of acute ischemic stroke. However, its use is limited by a narrow therapeutic window and only 3–8.5% of patients benefit from it [4]. With the exception of anti-thrombolytics (i.e., tissue plasminogen activator, tPA) and hypothermia, all therapies fail to reduce neuronal injury, neurological deficits, and mortality rates suggesting that the development of novel therapies against ischemic stroke is urgently needed.

Traditional Chinese medicine has a long history and rich clinical experience in the treatment and rehabilitation of ischemic stroke patients [5,6]. Artemisinin and its derivatives are among the most effective anti-malaria therapies, being used with great safety as first-line treatments [7]. Previous research has shown that artemisinin exerts a neuroprotective effect by being able to protect PC12 cells and cortical neurons from oxidative stress induced by hydrogen peroxide and sodium

---

nitroprusside (SNP) [8,9]. Artemether is an artemisinin derivative with a higher anti-malarial activity than artemisinin. This compound can easily pass through the blood-brain barrier and it is used more frequently in the clinic [10–12]. Besides its strong anti-malarial activity, it has also potential as an anti-cancer [13,14], anti-allergic or anti-inflammatory [15,16], anti-viral [17], anti-helminths and anti-protozoan parasitic [18,19] drug. In addition, several studies have also been reporting its potential use in oxidative stress suppression [8,9, 20,21]. Unfortunately, the protective effects and the molecular mechanism by which artemether affects ischemic stroke was not investigated.

ERK1/2 pathway is a key signal component and plays an important role in the activation and regulation of cell proliferation, cell survival and cell apoptosis [22]. Acute ischemic stroke injury is accompanied by changes in the intracellular signaling cascade involved in neuronal survival such as the ERK1/2 pathways [23,24]. Artemisinin was reported to protect RPE cells and neuronal cells against oxidative stress-induced apoptosis through ERK pathways which makes artemisinin and its derivatives as potential candidates for the ischemic stroke [8, 9]. A series of pathological events are occurring during acute ischemic stroke due to the loss of oxygen and energy supply, which results in irreversible neuronal and brain tissue damage [25]. Reactive oxygen species (ROS) accumulation has been described to be associated with brain injury after ischemic stroke [26]. The rapid increase of ROS production after acute ischemic stroke disrupts the endogenous antioxidant defense mechanisms, leading to tissue damage. ROS can destroy cell macromolecules, leading to autophagy, apoptosis and necrosis [27,28]. In addition, the rapid recovery of the blood flow increases tissues oxygenation levels, further increasing the production of ROS leading to reperfusion injury [29–31]. Therefore, it is very important to develop new therapeutic approaches that may lead to the reduction of oxidative damage. Artemisinin and artemether were reported to protect against oxidative stress-induced apoptosis in neurodegenerative disease *in vitro* and *in vivo* [32–34], further supporting the potential use of artemether in the treatment of ischemic stroke.

In this study, we assessed the protective effect of artemether in a classical middle cerebral artery occlusion (MCAO) stroke animal model and in an OGD/RP cellular model and found that artemether reduced cell injury by stimulation of the Erk1/2-P90rsk-CREB signaling pathway. These results provide evidences that artemether may play a critical role in the protection against cerebral ischemic injury supporting its potential use in the treatment of ischemic stroke.

## 2. Materials and methods

### 2.1. Materials

Monofilament nylon sutures were purchased from Beijing Sunbio Biotech Co. Ltd. (Beijing, China), 2,3,5-triphenyltetrazolium chloride (TTC, Cat# T8877) were obtained from Sigma Aldrich (St. Louis, MO, USA). Dulbecco's Modified Eagle's Medium (DMEM) with or without glucose, Fetal Bovine Serum (FBS), Bovine Serum Albumin (BSA) and 0.25% Trypsin were obtained from GIBCOTM (Invitrogen Corporation). 3-(4,5-dimethylthiazol-2-yl)-2,5-diphenyl tetrazolium bromide (MTT) and Hoechst 33,342 were purchased from Molecular Probes (Eugene, or, USA). Artemether (ARTE), BrdU (5-Bromo-2-deoxyuridine), Penicillin/ Streptomycin, Lipofectamine 2000 reagent, DMSO were purchased from Sigma Aldrich (St. Louis, MO, USA).Pierce BCA protein assay kit and HaltTM Protease and phosphatase inhibitor cocktail were purchased from Thermo Scientific (USA), Nissl staining solution, DCFH-DA reagent and 5,5′,6,6′-tetrachloro-1,1′,3,3′-tetraethyl-benzimidazolyl-carbocyanineiodide (JC-1) were ordered from Beyotime Institute of Biotechnology (Shanghai, China). Total superoxide dismutase (SOD) assay kit, lipid peroxidation malonaldehyde (MDA) assay kit and Caspase 3 activity detection kit, TUNEL Apoptosis Assay kit were obtained from Beyotime Institute of Biotechnology (Shanghai, China). LDH assay kit was obtained from Promega (USA).Annexin V-FITC/PI apoptosis

detection kit was obtained from BD Biosciences (San Diego, CA, USA). Anti-phospho-ERK1/2, anti-ERK1/2, anti-phospho-p90rsk, anti-phospho-CREB, anti-CERB, anti-cleaved caspase-3, anti-NeuN and anti-β-actin antibodies were purchased from Cell Signaling Technology (Woburn, MA, USA). Anti-Bax and anti-Bcl2 antibodies were purchased from Signalway Antibody (College Park, Maryland, USA), anti-BrdU, anti-Nestin were from Millipore (Darmstadt, Germany), biotinylated secondary antibody anti-rabbit IgG, TRITC-conjugated anti-rabbit IgG and FITC-conjugated anti-mouse IgG were purchased from Cell Signaling Technology, Woburn, USA), siERK1/2 were purchased from Genepharma (Shanghai, China), ERK1/2 inhibitor PD98059 was ordered from Calbiochem (San Diego, CA, USA).

### 2.2. Middle cerebral artery occlusion (MCAO) model

The experimental protocol was approved by the Animal Ethics and Welfare Committee of the University of Macau and was carried out in accordance with the approved guidelines and regulations. A total of 130 male C57 mice weighing 21–23 g were obtained from the Animal Research Core and housed under controlled temperature (24–26 °C), humidity and lighting (12-h light/dark cycle). Food and water were available *ad libitum* throughout the experiment. Mice were randomly divided into five groups (20 animals per group): blank group (healthy mice only exposed skin and blood vessels); MCAO model group and MCAO model plus artemether treatment groups (MCAO + artemether; 5, 10 and 20 mg/kg of artemether administered via intra-peritoneal during reperfusion). MCAO was performed according to previously described procedures [35]. Mice were anesthetized with an intra-peritoneal ininjection of 1% pentobarbital (40 mg/kg), placed on their back and an incision on the skin of the ventral neck was performed. The right common carotid artery (CCA) was exposed, and then the external carotid artery (ECA) and internal carotid artery (ICA) were separated. A monofilament nylon suture (diameter 0.21 mm) with a circular tip was inserted through the right external carotid artery (ECA) into the internal carotid artery (ICA) and moved forward slightly to occlude the left middle cerebral artery (MCA). Reperfusion was achieved by gently removing the monofilament until the tip cleared the ECA lumen after 1 h of occlusion. The body temperature was maintained at 37 ± 0.5 °C throughout the procedure. MCAO model was also established in male Sprague Dawley (SD) rats weighting 160–180 g using the same method. In short, after exposing and separating the right CCA, the ECA and ICA, the ECA was ligated and a monofilament nylon suture (diameter 0.31 mm) was inserted into ICA until resistance was encountered to prevent the origin of the middle cerebral artery. Cerebral blood flow (CBF) was measured in the area of the MCA by a laser doppler flowmetry (RWD, Shenzhen, China) and the detector was fixed on the skull above the cortex. All animals received humane care in compliance with the Guide for the Care and Use of Laboratory Animals published by the National Institute of Health.

### 2.3. Neurological evaluation

Neurological deficit scores were evaluated by an observer blinded to the experimental groups. Zea-Longa Scale was used to assess the neurological function of MCAO models as previously described [36]: grade 0, normal (no apparent neurological deficits); grade 1, failure to entirely extend the contralateral forelimb; grade 2, circling continuously to the contralateral side but standard posture at rest; grade 3, falling to the injured side; grade 4, no spontaneous autonomic activity and a sluggish level of consciousness; grade 5, death. Animals with grades of 0, 1 or 5 were withdrawn from the study.

### 2.4. Grip strength and sensory function measurement

A grip strength meter (Bioseb, USA) and a hot plate (Panlab Harvard Apparatus, Barcelona) were used to assess the grip strength and the

recovery of the sensory function of the animals at days 1, 3, 7, 14 and 28 after MCAO. The assays were performed as previously reported [37,38]. Briefly, for the measurement of the grip strength, the animal's forelimbs were placed on the grid of the grip strength meter. The animals were then pulled away from the grid until losing the grip. The grip strength of each animal was displayed on the screen and recorded. The hot plate test has been widely used to assess the sensory function by measuring the thermal withdrawal latency (the latency of paw licking) of the forelimbs. Briefly, the surface of the hot plate apparatus was set to 50 °C, and then the animals were gently lifted by the tail, so that their forelimbs touched the plate surface. The latency of paw licking was recorded.

### 2.5. Morris water maze test

The MWM was used to test the learning and memory abilities of the animals 1 month after the surgical procedures. The assays were performed as reported previously [39] and included a 4-day hidden platform test and a 1-day spatial probe test. Briefly, the animals were allowed to swim for 60 s before getting to the platform for the hidden platform test. The time to reach the platform (escape latency) was recorded. Then, the spatial probe test was carried out 24 h after the last time of the hidden platform test and the percentage of time spent on the target quadrant and the number of crossings in the target quadrant area were measured.

### 2.6. Tissue samples preparation

Animals were sacrificed 24 h after MCAO procedure by decapitation and the brains were immediately extracted. Brains used for TTC staining were immediately used, brains used for SOD, MDA and western blotting analysis were immediately used or stored in −80 °C. Brains used to determine the water content were immediately weighed after dissection and dried for 48 h. Brains used for HE Staining, Nissl Staining, TUNEL assay, immunofluorescence and immunohistochemical analysis were post-fixed overnight in 4% paraformaldehyde (PFA). After fixation, the samples were dehydrated and embedded in paraffin using standard methods [32]. Coronal 4 $\mu$m sections were cut and kept at 37 °C for 24 h, followed by deparaffination and hydration.

### 2.7. 2, 3, 5-triphenyltetrazolium chloride (TTC) staining

TTC (2,3,5-triphenyltetrazolium chloride) staining was used to evaluate the size of the infarct volume in MCAO model groups. Coronal brain sections (2 mm) were put into 2% TTC stain in saline at 37 °C and gently stirred to ensure an homogeneous staining exposure for 15 min. Excess TTC was drained off, and the slices were fixed in 4% PFA during overnight. TTC stained and post-fixed brain slices were then scanned by a photo scanner. TTC stains viable brain tissue in deep red and the infarcted tissue remains unstained. Infarct and total brain volumes were quantified with an Image J analysis system. Brain infarct volume was expressed as a percentage of total brain tissue volume. All studies were performed for a minimum of 5 sections per sample, with 5 animals in each group.

### 2.8. Brain water content

We observed brain water content using the wet–dry method [40,41]. The right hemisphere of the dissected brains was immediately collected and weighed (wet tissue weight) 24 h after MCAO. Afterwards, the brain samples were dried in an oven at 95 °C for 48 h and weighed again (dry tissue weight). The brain water content was calculated as [(wet tissue weight − dry tissue weight)/wet tissue weight] × 100% (4 animals per group).

### 2.9. HE staining, Nissl Staining and TUNEL assay

HE and Nissl stainings were conducted according to routine protocols [32]. Nissl staining was used to detect surviving neurons. The survival index was calculated as follows: survival index (%) = (number of surviving neurons/total number of neurons) × 100%. The apoptotic response was assessed by TUNEL assay using the commercially available TUNEL Apoptosis Assay kit (Beyotime Institute of Biotechnology, Shanghai, China). The assay was performed according to the instructions provided by the manufacturer. The apoptosis index in the peri-infarct region was calculated as follows: apoptosis index (%) = (number of apoptotic neurons/total number of neurons) × 100%. All studies were performed for a minimum of 5 sections per sample, with 4 animals in each group.

### 2.10. BrdU labelling

Animals from each group received intraperitoneal injections of BrdU (50 mg/kg/time) with an interval of 2 h from reperfusion to sacrifice. To detect BrdU-labeled cells, brain sections were subjected to double immunofluorescence labeling for BrdU and NeuN. Following incubation with primary antibodies (Rabbit anti-NeuN, 1:500; mouse anti-BrdU, 1:500), the corresponding secondary antibody was used for NeuN (TRITC-conjugated anti-rabbit IgG, 1:500) and BrdU (FITC-conjugated anti-mouse IgG, 1:500). The images were captured with a fluorescence microscope (Nikon A1 confocal microscope). All studies were performed for a minimum of 5 sections per sample, with 3 animals in each group.

### 2.11. Immunofluorescence and immunohistochemical analysis

Immunofluorescence and immunohistochemical analyses were performed as previously described [32]. Briefly, after incubation with antigen retrieval solution and 3% $H_2O_2$ for 30 min, the slides were rinsed with PBS and incubated with the primary antibodies (Rabbit anti-Nestin, 1:500, Mouse anti-Brdu,Rabbit anti-NeuN) overnight at 4 °C. For negative controls, the primary antibody was replaced by nonimmunized serum. The following day, the slides were rinsed and incubated with the corresponding secondary antibody (TRITC-conjugated anti-rabbit IgG and FITC-conjugated anti-mouse IgG) for 1 h followed by three washes in PBS for 15 min. Nuclei were counterstained with 4′,6-diamidino-2-phenylindole (DAPI), and images were acquired with a Nikon A1 confocal microscope. For IHC analysis, the slides were incubated with biotinylated secondary antibody anti-rabbit IgG (1:500) at room temperature for 2h, processed using the avidin-biotin complex (Boster Biological Technology, Wuhan, China) and stained with 3,3′-diaminobenzidine (DAB) and hematoxylin. The slides were then examined and photographed using a microscope (EVOS FL Imaging System). All studies were performed for a minimum of 5 sections per sample, with 4 animals in each group.

### 2.12. Determination of superoxide dismutase, malonaldehyde

Brain samples were processed with a immunoprecipitation assay (RIPA) lysis buffer. Total superoxide dismutase (SOD) assay kit and lipid peroxidation malonaldehyde (MDA) assay kit were used to measure SOD, MDA contents, respectively. The assays were performed according to the instructions provided by the manufacturers (4 animals per group).

### 2.13. Cell culture

PC12 cells were obtained from the Cell Bank of Sun Yat-sen University (Guangzhou, China). The cells were grown in DMEM Dulbecco's Modified Eagle's Medium supplemented with 10% fetal bovine serum (FBS), 100 µg/ml streptomycin and 100 units/ml penicillin, and maintained at 37 °C in an humidified atmosphere of 5% $CO_2$.

Primary cultured cortical neurons were prepared from brains of
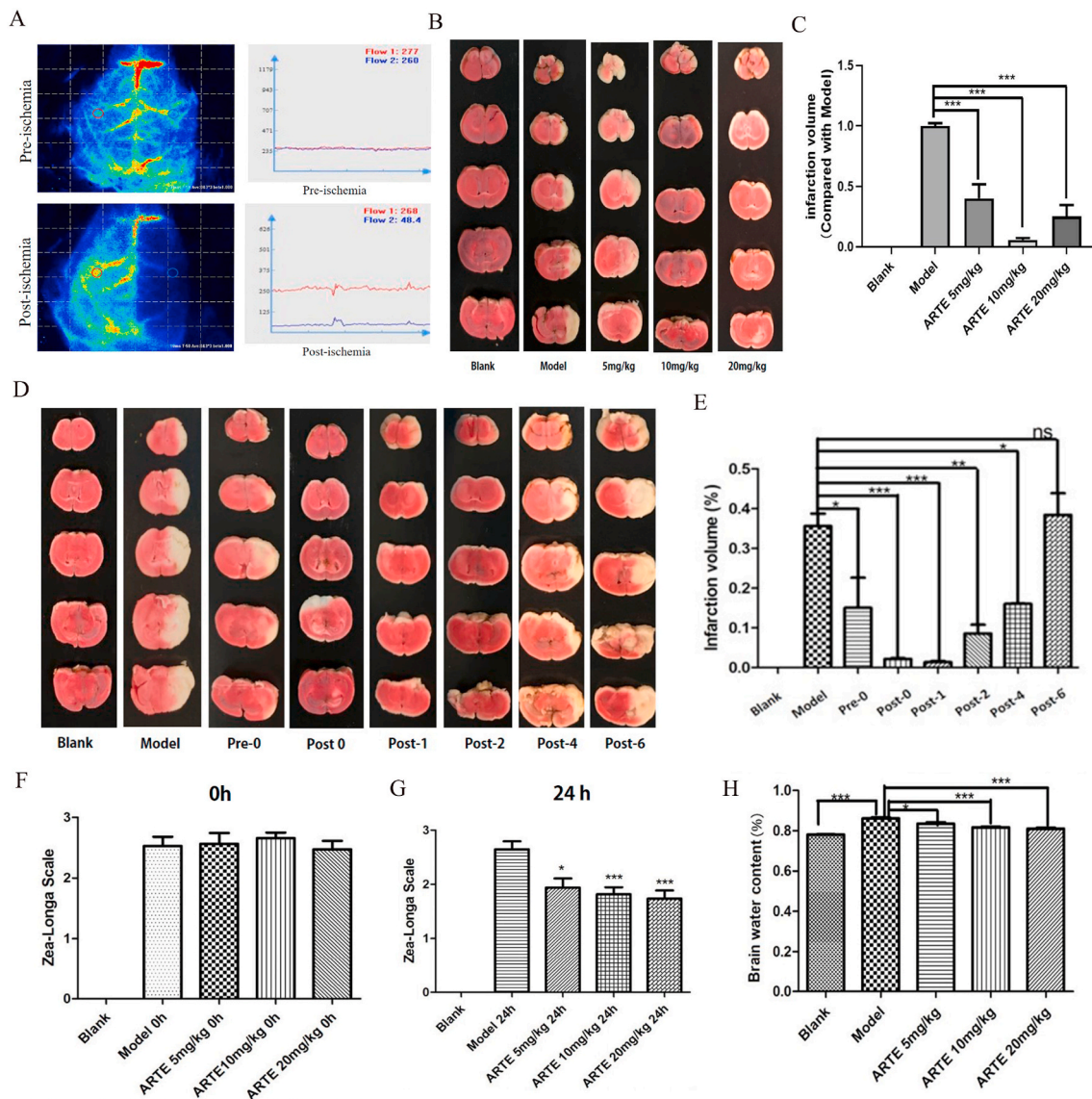
**Fig. 1.** Artemether attenuated the infarction volume, improved the neurological function and reduced the brain water content induced by MCAO. Mice were subjected to ischemia for 1 h and reperfusion for 24 h. Cerebral blood flow (CBF) was measured pre- and post-ischemia. After the model was established, the blood flow on the ischemic side (blue line) decreased about 82% when compared with the non-ischemic side (red line) (A). Artemether (5, 10 and 20 mg/kg) was administered 1 h after ischemia. TTC staining was performed to evaluate the infarction volume. Representative images of TTC stained brain slices indicating brain infarction at 24 h after MCAO and treatment with different concentrations of artemether (B). Quantification of the infarction volume of B (C). Representative images of TTC stained brain slices indicating brain infarction at different time points of artemether (10 mg/kg) treatment after MCAO (D). Quantification of the infarction volume of D (E). The neurological function was evaluated before artemether treatment (F) and 24 h after MCAO (G). The brain water content of each experimental group was measured 24 h after MCAO (H). *p < 0.05, **p < 0.01, ***p < 0.001 were considered significantly different. (For interpretation of the references to colour in this figure legend, the reader is referred to the Web version of this article.)

newborn C57BL/6 mice as previously described [42], and cultured for 7–8 days in neurobasal medium supplemented with 2% B27, 10 U/ml penicillin, and 10 μg/ml streptomycin at 37 °C in 5% $CO_2$ humidified atmosphere.

### 2.14. Establishment of OGD/RP model

For OGD treatment, cells were rinsed once with warm glucose-free DMEM (Gibco), and then placed in an incubator loaded with mixed gas containing 5% $CO_2$, 1% $O_2$ and 94% $N_2$ for 2 h, 4 h, 6 h and 8 h at 37 °C before reperfusion (re-oxygenation). For reperfusion, cells were refreshed with normal culture medium for 22 h, 20 h, 18 h and 16 h at 37 °C in an atmosphere of 5% $CO_2$, 21% $O_2$ and 74% $N_2$. Control groups were incubated in glucose-containing DMEM with equal refreshment at

37 °C in an atmosphere of 5% $CO_2$, 21% $O_2$ and 74% $N_2$ all the time.

### 2.15. MTT assay

Cells viability was assessed using MTT assay according to the commonly used protocols in our laboratory [43,44]. Cells were seeded in 96-well plates ($5x10^3$ cells/well) with 0.5% FBS. After exposure of cells to 2 h, 4 h, 6 h and 8 h of OGD followed by 22 h, 20 h, 18 h and 16 h of reperfusion, cell viability was measured by MTT assay after 24 h. To assess the effect of artemether pre-treatment, Cells were seeded in 96-well plates ($5x10^3$ cells/well) with 0.5% FBS and were pretreated with different concentrations of artemether (10–100 μM) or 0.1% DMSO for 2 h before OGD. After 4 h of OGD, cells were refreshed with normal culture medium and cell viability was tested by MTT assay 24 h later.
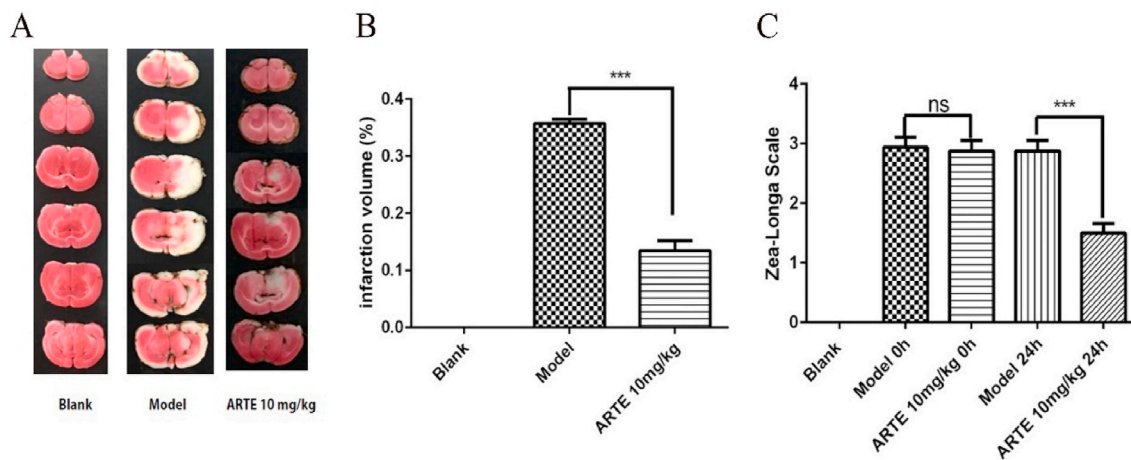
**Fig. 2.** Artemether attenuated the infarction volume and improved the neurological function in SD rats after MCAO. (A, B) Representative images of TTC stained brain slices indicating brain infarction in SD rats after MCAO and 10 mg/kg artemether treatment and quantification. (C) The neurological function was evaluated before and 24 h after artemether treatment. ***p < 0.001 were considered significantly different.

Cells were incubated with MTT (0.5 mg/mL) for 3 h at 37 °C. After this period, the medium is drawned and substituted by DMSO (100 μL). The absorbance at 570 nm was measured by BIO-RAD680 microplate reader (Thermo Fisher, MA, USA). The experiment was repeated 3 times.

### 2.16. Measurement of LDH

Cells cytotoxicity was evaluated by measuring the activity of lactate dehydrogenase (LDH) released into the medium according to commonly used protocols in our laboratory [42,43]. Briefly, cells were seeded into 96-well plates (1x10$^4$ cells/well). After artemether or DMSO treatments, the activity of LDH released into the medium was determined using Cyto Tox-ONETM Homogeneous Membrane Integrity Assay (Promega, USA), according to the instructions of the manufacturer. Fluorescence intensity was measured using an Infinite M200 PRO multimode microplate at excitation at 560 nm and emission at 590 nm wavelengths. The released LDH values were normalized to the percentage of the control group.

### 2.17. Caspase 3 activity detection

The activity of caspase 3 was measured as previously described [43, 44]. Briefly, after artemether treatment, the cells were extracted with lysis buffer and detection solution (sample: lysis buffer: Ac-DEVD-pNA = 5:4:1) was added followed by 2 h incubation. The absorbance was recorded at 405 nm using a BIO-RAD680 microplate reader (Thermo Fisher). All values of caspase 3 activity (%) were normalized to the control group.

### 2.18. Measurement of reactive oxygen species (ROS), mitochondrial membrane potential (△ψm) and cell apoptosis

These experiments were measured as previously described [42,43]. Intracellular reactive oxygen species (ROS) production was assessed by DCFH-DA reagent, according to the instructions of the manufacturer. Mitochondrial function, a pivotal indicator of cell health, can be evaluated by monitoring changes in mitochondrial membrane potential (△ψm) using JC-1 dye. In healthy cells, the dye accumulates in the mitochondria as red fluorescent aggregates. In apoptotic cells, the dye is converted to green fluorescent monomers and remains in the cytoplasm. Therefore, the red/green fluorescence ratio can be used to determine the mitochondrial function of OGD-induced cells with or without pre-treatment with artemether. The number of apoptotic cells was measured by flow cytometry and Hoechst 33342 staining. Each

experiment was repeated three times.

### 2.19. Western blotting

Western blotting was performed as previously described [32,43]. Cells or brain tissues were lysed in radioimmunoprecipitation assay (RIPA) buffer supplemented with a protease and phosphatase inhibitor. Protein concentration was measured using a BCA protein assay kit (Thermo scientific), according to the manufacturer's instructions. Proteins were resolved by SDS-PAGE (polyacrylamide gel electrophoresis) and transferred to polyvinylidene fluoride (PVDF) membranes. Membranes were blocked in 5% non-fat milk in PBST for 1 h and probed with selective primary antibodies (Bcl2, Bax, Cleaved Caspase 3, P-ERK, T-ERK, P–P90$^{rsk}$, P-CREB, T-CREB at a 1:1000 dilution, actin, GAPDH at a 1:1500 dilution) overnight at 4 °C. Membranes were washed and incubated with horseradish peroxidase conjugated anti-rabbit secondary antibody (CST) at a dilution of 1:5000 for 1 h at room temperature. Immunoblotting was performed using an ECL detection kit reagent.

### 2.20. ERK1/2 silencing by siRNA

Gene silencing of ERK1/2 was performed as previously described with minor modifications [45]. Interfering RNA (siRNA) were synthesized by GenePharm (Shanghai). The sequence of ERK1 gene was 5′-GGCCUCAAGUACAUACACUTT AGUGUAUGUACUUGAGGCCTT-3'; and the sequence of ERK2 gene was 5′-CCUGAGAGGAUUAAAGUAUTT AUACUUUAAUCCUCUCAGGTT-3'. Briefly, PC 12 cells were cultured in DMEM medium containing with 10% FBS plus antibiotics, and were maintained at 37 °C in a humidified, 5% CO2 atmosphere. The next day, cells were transfected with specifically synthesized siRNA or scrambled siRNA using Lipofectamine 2000 for 6 h. Then, media was replaced with DMEM plus 10% serum for 48 h, cells were collected for protein expression analyses or MTT assays.

### 2.21. Statistical analysis

All the data are presented as mean ± SEM. Each experiment was performed in triplicates. Statistical differences were analyzed by one-way ANOVA (Analysis of variance) in combination with a post-hoc test, and p values < 0.05 were considered statistically significant.
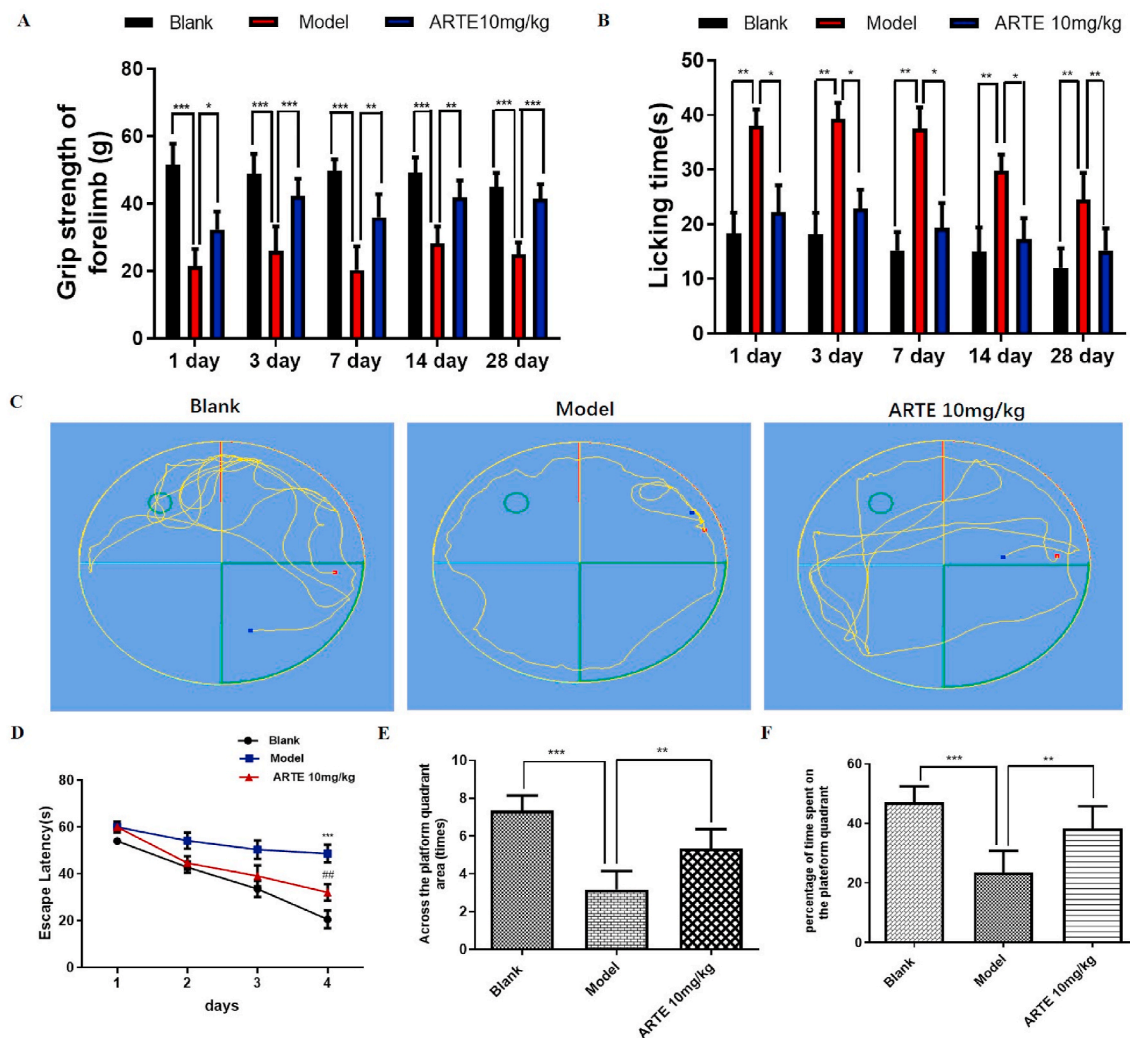
**Fig. 3.** Artemether improved the grip strength, the recovery of sensory function and the learning and memory abilities in C57 mice after MCAO. (A) The grip strength was evaluated at days 1, 3, 7, 14 and 28. During this period, the animals were treated with 10 mg/kg artemether once a day. Artemether significantly improved the grip strength of treated animals in comparison with the model group; *$p < 0.05$, **$p < 0.01$, ***$p < 0.001$ were considered significantly different. (B) The recovery of the sensory function was evaluated at the same time intervals. Artemether treatment significantly improved the recovery of sensory function of treated animals in comparison with the model group; *$p < 0.05$, **$p < 0.01$ were considered significantly different. (C) Representative images of each group of Morris water maze test. (D) Escape latency results of the Morris water maze test. Artemether treatment decreased the escape latency in comparison with the model group; ***$p < 0.001$, versus Blank group; ###$p < 0.001$ versus Model group were considered significantly different. (E) Number of crosses in the target quadrant in the Morris water maze test. Artemether treatment increased the number of crosses in the target quadrant in comparison with the model group, **$p < 0.01$, ***$p < 0.001$ were considered significantly different. (F) Percentage of time spent on the target quadrant of Morris water maze test. Artemether treatment increased the percentage of time spent on the target quadrant in comparison with the model group. **$p < 0.01$, ***$p < 0.001$ were considered significantly different.

## 3. Results

### 3.1. Artemether attenuated the infarction volume in MCAO model

TTC staining is a commonly used indicator for evaluating cerebral ischemic injury [46]. Analysis of the stained coronal brain sections revealed that artemether treatment significantly reduced the cerebral ischemia infarction volume in MCAO mice in a dose dependent manner (Fig. 1B and C). Temporal analysis revealed that the neuroprotective effect of artemether, at a dose of 10 mg/kg, is delimited by a therapeutic window that ranges from 0 to 4 h post ischemia (Fig. 1D and E). Moreover, the neuroprotective effect of artemether was also present in MCAO rat model. Artemether (10 mg/kg) treatment significantly improved the cerebral ischemia infarction volume of rats with cerebral ischemic injury (Fig. 2 A, B).

### 3.2. Artemether improved the neurological deficits and reduced brain edema in MCAO mouse model

The neurological deficits were evaluated before and 24 h after artemether administration. Results revealed that artemether treatment significantly improved the neurological deficits of MCAO mice and rats, as measured using Zea-Longa scale, 24h after reperfusion (Fig. 1F and G and Fig. 2C). Assessment of the brain water content revealed that MCAO mice presented significantly increased brain water contents when compared with the animals from the control group. Artemether treatment significantly reduced the brain edema when compared with the MCAO model animals (Fig. 1H).

### 3.3. Artemether improved the grip strength, the recovery of sensory function and the learning and memory abilities in C57 mice after MCAO

The grip strength and the recovery of the sensory function were
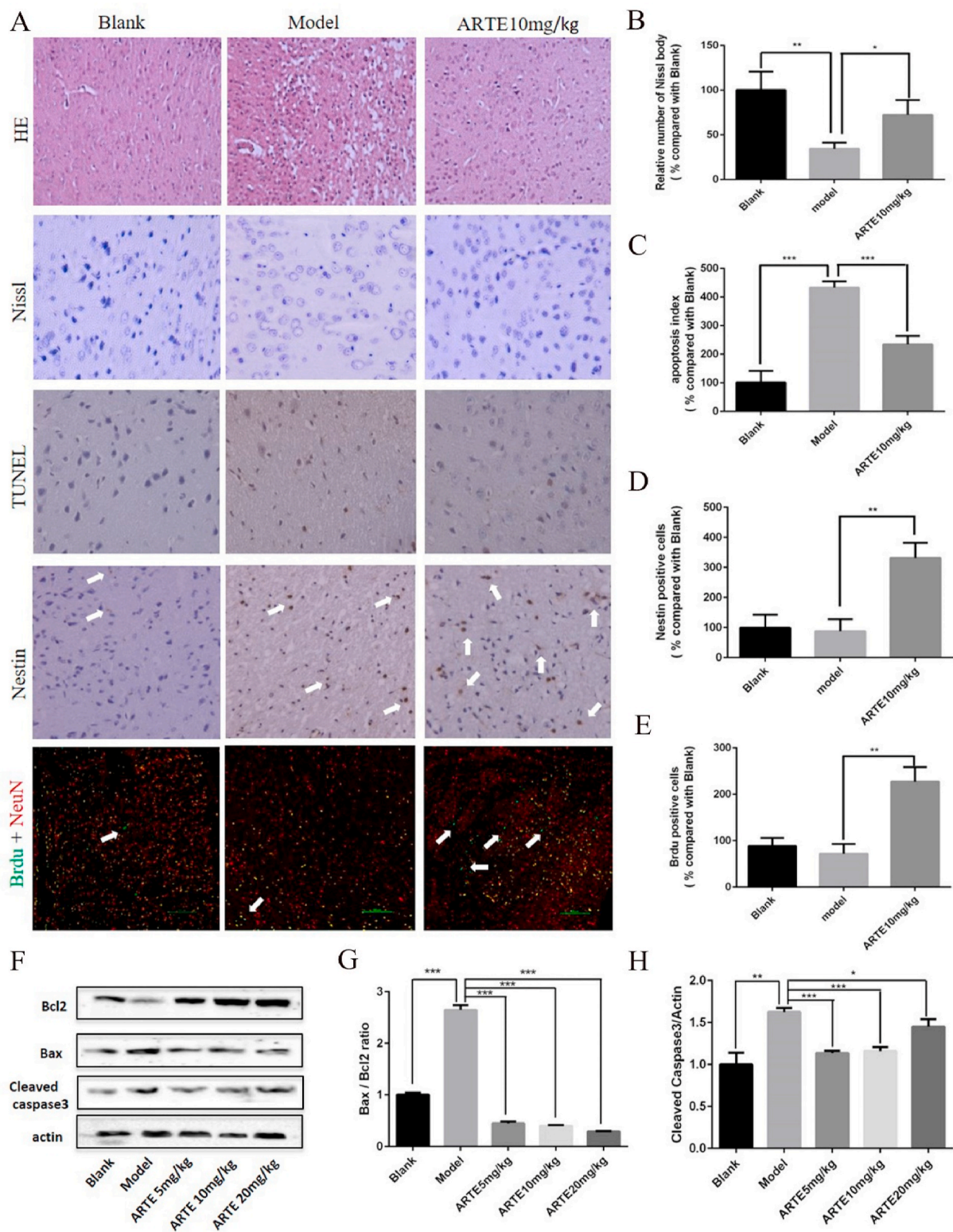
**Fig. 4.** Artemether attenuated cell injury and promoted cell proliferation after MCAO. (A) Representative images of HE, Nissl, TUNEL assay, Nestin and Brdu + NeuN stained brain sections. (B, C, D, E) Quantification of Nissl bodies staining, TUNEL assay, immunohistochemistry and immunofluorescence results. (F) Bax, Bcl2 and cleaved caspase 3 protein expression levels in each group was detected by western blotting. (G, H) Quantification of the western blotting data. Three independent experiments were performed in triplicate. *p < 0.05, **p < 0.01, ***p < 0.001 were considered significantly different.

evaluated at days 1, 3, 7, 14 and 28 after artemether treatment. Obtained results revealed that artemether treatment significantly improved the grip strength and the recovery of sensory function of MCAO mice after reperfusion (Fig. 3A and B). Assessment of the learning and

memory abilities one month after the surgical procedure, revealed that MCAO mice presented learning and memory deficits when compared with the animals from the blank group. Artemether treatment for one month significantly attenuated the learning and memory deficits when
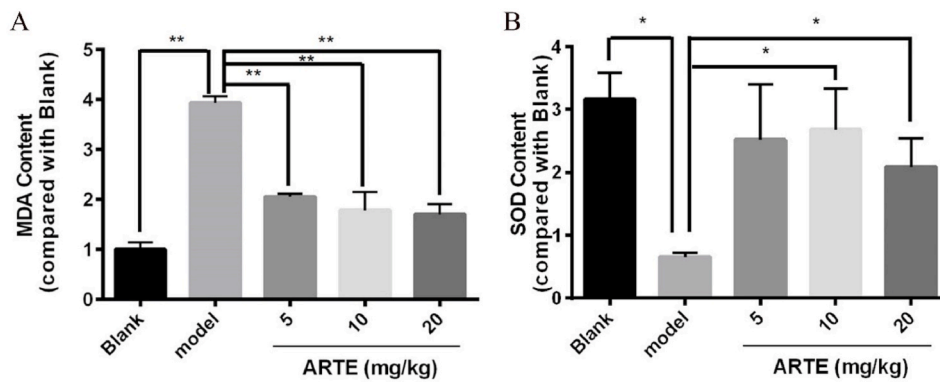
**Fig. 5.** Artemether decreased the levels of malonaldehyde (MDA) and increased the levels of superoxide dismutase (SOD) after MCAO. (A) The levels of malonaldehyde (MDA) and (B) superoxide dismutase (SOD) were determined using an enzyme-linked immunosorbent assay. Three independent experiments were performed in triplicate. *p < 0.05, **p < 0.01 were considered significantly different.

compared with the MCAO model animals as denoted by the decrease of the escape latency and by the increase of the percentage of time spent on the target quadrant and the number of crossings in the target quadrant area presented by treated animals in comparison with the MCAO model animals (Fig. 3D–F).

### 3.4. Artemether attenuated MCAO- induced cell injury

Morphological analysis revealed that MCAO caused neuronal vacuolar degeneration that was reduced by artemether treatment (10 mg/kg) (Fig. 4A-HE). MCAO also induced alterations in the number of Nissl bodies in the peri-infarct region. Specifically, it induced a significant decrease in the number of Nissl bodies compared to control animals that was reversed by artemether treatment (10 mg/kg) (Fig. 4A-Nissl, B). MCAO mice also presented a significantly higher number of TUNEL-positive cells in the peri-infarct region, an increased Bax/Bcl-2

expression ratio and cleaved caspase 3 expression level when compared to control animals. The number of apoptotic cells was significantly decreased by the treatment with artemether (10 mg/kg) (Fig. 4A-TUNEL, C). The MCAO-induced increase of Bax/Bcl-2 expression ratio and cleaved caspase 3 expression level were also significantly decreased upon artemether treatment (5,10 and 20 mg/kg) (Fig. 4F–H).

### 3.5. Artemether promoted neuronal proliferation in MCAO mouse model

Artemether treatment (10 mg/kg) significantly increased the expression levels of the neural stem cell marker (nestin) in the brain peri-infarct region (Fig. 4A-Nestin, D). Further assessment of BrdU/NeuN positive neurons revealed that artemether treatment (10 mg/kg) promoted the neuronal proliferation in this area (Fig. 4A-Brdu + NeuN, E).
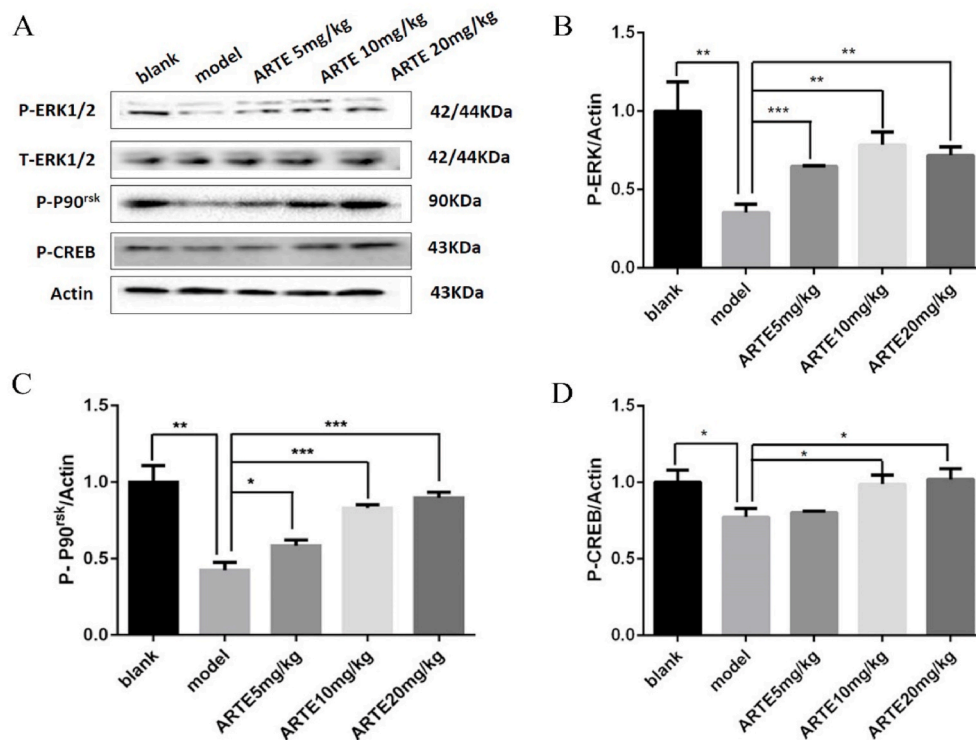


**Fig. 6.** Artemether stimulated the phosphorylation of Erk1/2-P90$^{rsk}$-CREB after MCAO. (A) The phosphorylation of ERK, P90$^{rsk}$ and CREB was detected by western blotting. (B, C, D) Quantification of western blotting results. Three independent experiments were performed in triplicate. *p < 0.05, **p < 0.01, ***p < 0.001 were considered significantly different.
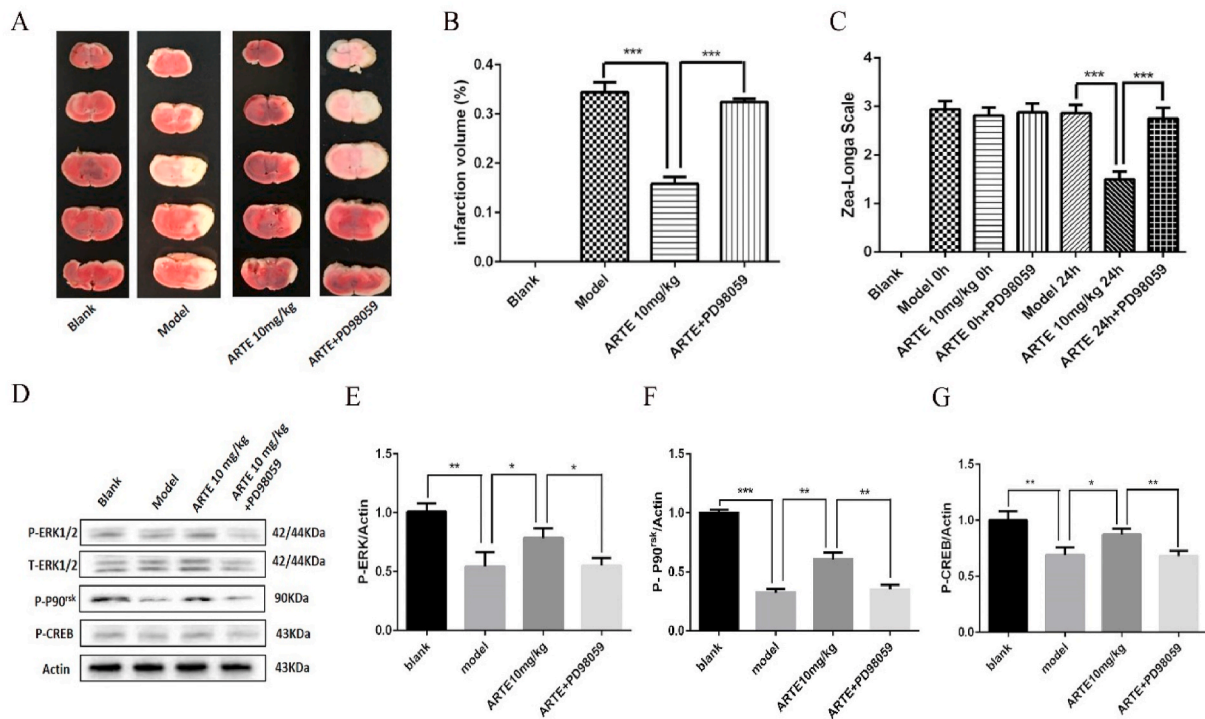
**Fig. 7.** The neuroprotective effect of artemether is blocked by PD98059. Effect of ERK inhibitor PD98059 pre-treatment on artemether (10 mg/kg) neuroprotective action on MCAO. (A, B) Representative images of TTC stained brain slices indicating brain infarction areas and quantification. (C) Evaluation of the neurological function was performed before and 24h after ERK inhibitor PD98059 and artemether treatments.(D) Phosphorylation of ERK, P90$^{rsk}$ and CREB were detected by western blotting. (E, F, G) Quantification of the western blotting results. Three independent experiments were performed in triplicates. *p < 0.05, **p < 0.01, ***p < 0.001 were considered significantly different.

### 3.6. Artemether attenuated MCAO-induced oxidative stress

Lipid oxidation occurs whenever oxidative stress occurs. MDA is a natural product of lipid oxidation in organisms, so it can be used to detect lipid oxidation levels. The results revealed that the MDA levels were significantly increased in the brains of MCAO model group. Upon artemether treatment (5, 10, 20 mg/kg), MDA levels significantly decreased (Fig. 5A). In contrast, assessment of SOD contents revealed that the level of SOD was significantly decreased in the brain of MCAO model group. Artemether treatment induced a significant increase of SOD contents in the brains of MCAO animals (Fig. 5B).

### 3.7. Artemether stimulated Erk1/2-P90$^{rsk}$-CREB signaling pathway in MCAO mouse model and this effect was blocked by PD98059

Previous studies reported that up-regulation of ERK 1/2 signaling activity has a positive neuroprotective effect in ischemia stroke *in vivo* and *in vitro* models [47,48-50]. In this study, MCAO induced a down-regulation of the phosphorylation of ERK1/2, P90$^{rsk}$ and CREB, the downstream proteins of ERK1/2. Upon artemether treatment the phosphorylation levels of ERK1/2, P90$^{rsk}$ and CREB significantly increased (Fig. 6). Moreover, animals pretreatment with the ERK1/2 inhibitor PD98059, resulted in the inhibition of the neuroprotective effect of artemether on the infarction volumes (Fig. 7A and B) and neurological deficits (Fig. 7C), with an apparent direct correlation with the down-regulation of Erk1/2-P90$^{rsk}$-CREB signaling activities (Fig. 7D–G).

### 3.8. Artemether attenuated OGD/RP-induced cell cytotoxicity

OGD conditions during 4, 6 and 8 h induced a significant decrease in the cells viability compared with the control group. Attending to the significant impact of OGD conditions for 4 h followed by 20 h of reperfusion on cell viability (~60%), this protocol was selected to

establish the OGD/RP model in all the experiments (Fig. 8A). Assessment of the possible neuroprotective effect of artemether on OGD/RP-induced cell death revealed that artemether pre-treatment improved cell viability in a dose-dependent manner (10–100 μM) (Fig. 8B). Measurement of LDH release, Caspase 3 activity, MDA and SOD contents revealed that artemether (30 μM) confered neuroprotection towards OGD/RP-induced necrotic cell death, cell apoptosis and oxidative stress (Fig. 8C–F).

### 3.9. Artemether reduced intracellular ROS, reversed mitochondrial membrane potential (△ψm) and decreased cell apoptosis in OGD/RP-induced cell injury

Cells exposure to OGD for 4 h and reperfusion for 20 h induced a significant increase in the production of intracellular ROS and a significant decrease of cells mitochondrial membrane potential compared with control cells that were reversed by artemether pre-treatment (10–100 μM) (Fig. 9A–C). Further investigation of the neuroprotective effect of artemether upon OGD/RP-induced apoptosis, revealed that artemether pre-treatment (10–100 μM) significantly reversed the OGD/RP-induced increase of cell apoptosis (Fig. 9D and E). In accordance with these nuclei morphological changes, FACS analyses of Annexin-V-FITC labeled cells also indicated that artemether inhibited OGD/RP-induced apoptosis. Furthermore, the OGD/RP -induced increase of Bax/Bcl-2 expression ratio was also decreased upon artemether pre-treatment with different concentrations (Fig. 9H and I).

### 3.10. Erk1/2-P90$^{rsk}$-CREB signaling pathway is involved in the neuroprotective effect of artemether on OGD/RP-induced cell injury

Assessment of the involvement of Erk1/2-P90$^{rsk}$-CREB signaling pathway in the neuroprotective effect of artemether on OGD/RP-induced cell injury, revealed that similarly to the MCAO experimental
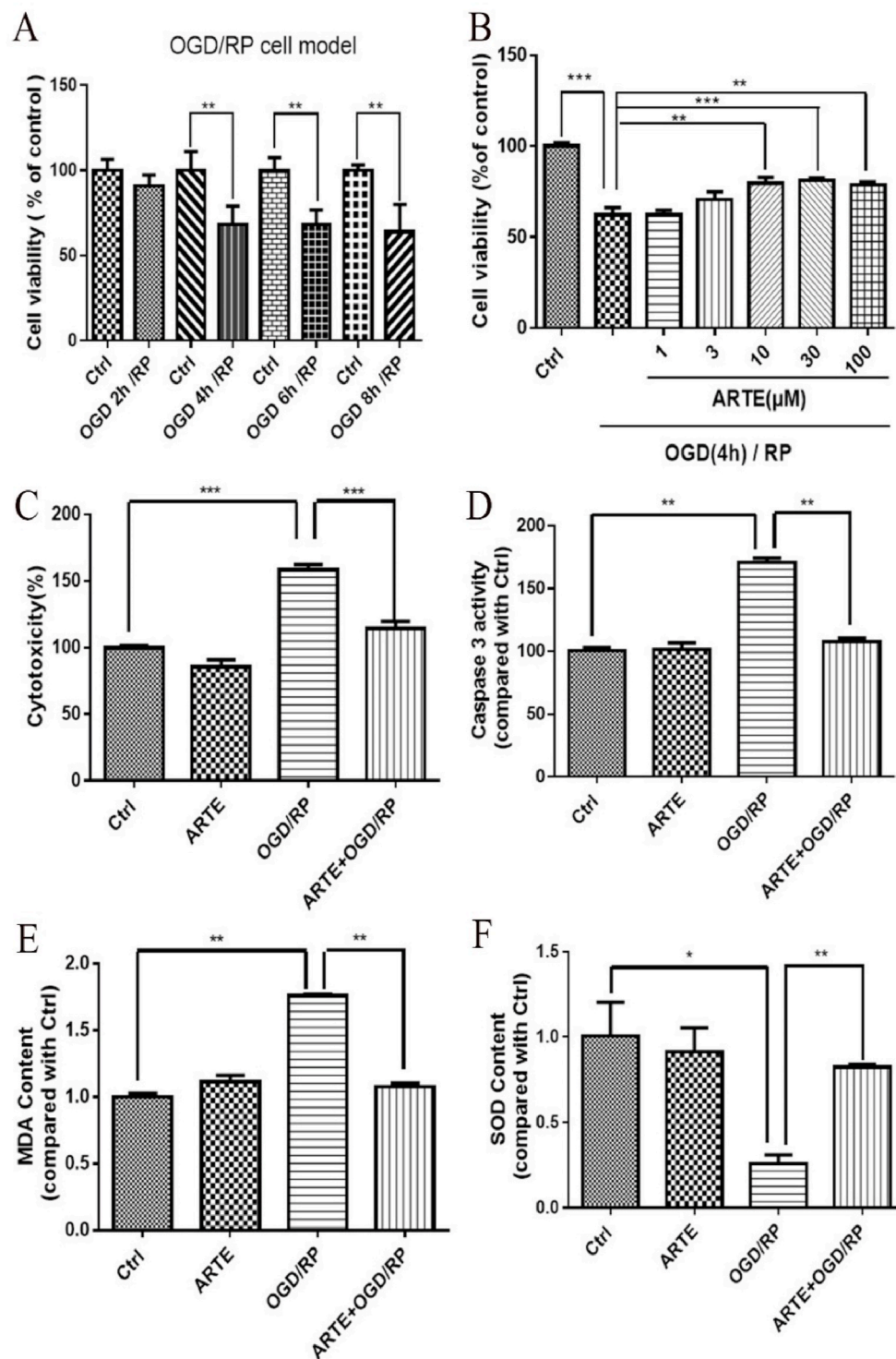
**Fig. 8.** Artemether attenuated OGD/RP-induced cell injury in PC12 cells. (A) Viability of PC12 cells exposed during 2, 4, 6 and 8 h to OGD conditions followed by 22, 20, 18 and 16 h of reperfusion. (B) Cells were pre-treated with varying concentrations of artemether or 0.1% DMSO (vehicle control) for 2 h and then incubated with or without OGD conditions for 4 h followed by 20 h of reperfusion. Cell viability was measured by MTT assay. (C) PC12 cells were pre-treated with artemether (30 μM) for 2 h and then incubated with or without OGD for additional 4 h followed by 20 h of reperfusion. Cells cytotoxicity was assessed by LDH release assay. (D) Measurement of Caspase 3 activity. (E,F) Measurement of malonaldehyde (MDA) and superoxide dismutase (SOD) levels. Three independent experiments were performed in triplicate. *p < 0.05, **p < 0.01, ***p < 0.001 were considered significantly different.

model, artemether pre-treatment also induced a significant increase in the phosphorylation of ERK1/2, P90$^{rsk}$ and CREB (Fig. 10). In addition, the neuroprotective effect of artemether in the cells injured by OGD/RP was blocked upon inhibition of ERK1/2 with PD98059 (Fig. 11A). Knock-down of ERK1/2 further validated these findings as it robustly eliminated the cell protective tendency of artemether (Fig. 11B and C). Additional experiments revealed that treatment of cells with PD98059 prevented artemether-induced decrease of intracellular ROS and cell apoptosis and reversal of mitochondrial membrane potential (△ψm) (Fig. 11D–G).

### 3.11. Artemether conferred neuroprotection against OGD/RP induced cell injury in primary cultured cortical neurons

The possible neuroprotective effect of artemether on OGD/RP-induced cell injury in primary cultured cortical neurons was assessed. MTT results revealed that artemether pre-treatment improved cell viability in a dose-dependent manner (3–30 μM) (Fig. 12A) and that this neuroprotective effect was blocked upon inhibition of ERK1/2 with PD98059 (Fig. 12B). Measurement of LDH release revealed that artemether (10 μM) conferred neuroprotection towards OGD/RP-induced
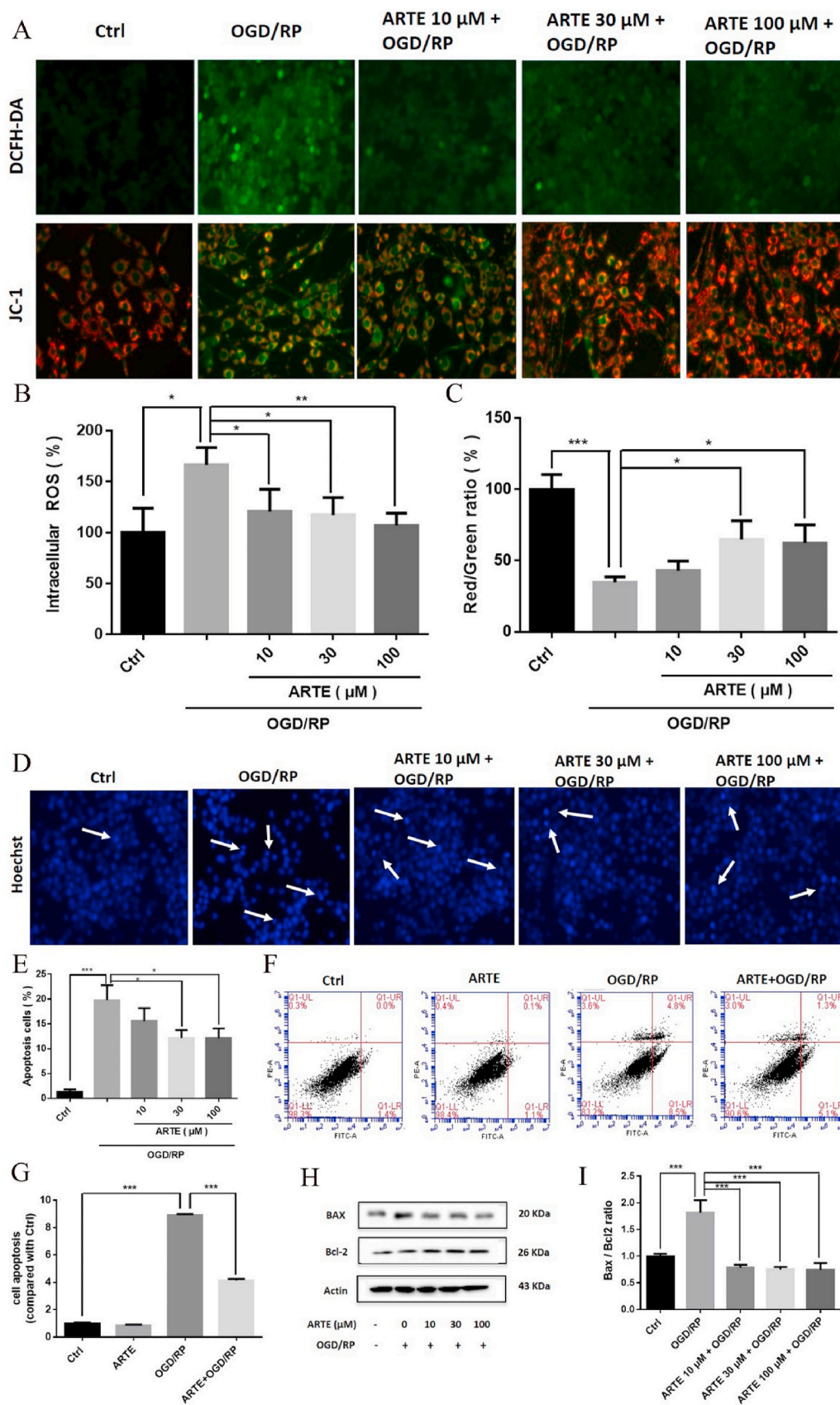
**Fig. 9.** Artemether decreased mitochondrial membrane potential, the production of ROS and cell apoptosis in PC12 cells exposed to OGD/RP conditions. PC12 cells were pre-treated with varying concentrations of artemether or 0.1% DMSO (vehicle control) for 2 h and then incubated with or without OGD conditions for 4 h followed by 20 h of reperfusion. (A) Representative images of DCFH-DA assay and of cells stained with JC-1 dyes depicting intracellular ROS and the changes of mitochondrial membrane potential ($\triangle \psi m$), respectively. (B) Quantification of intracellular ROS levels. (C) Quantification of the red to green fluorescence intensity ratio representing the loss of mitochondrial membrane potential. (D) Representative images of Hoechst 33,342 staining. The apoptotic cells with condensed chromatin are indicated by an arrow head. (E) Quantification of apoptotic cell's nuclei. (F,G) Determination of cell apoptosis by flow cytometry. (H) Bcl-2 and Bax levels were detected by western blotting. (I) Quantification of Bax/Bcl-2 ratio. Three independent experiments were performed in triplicate. *p < 0.05, **p < 0.01, ***p < 0.001 were considered significantly different. (For interpretation of the references to colour in this figure legend, the reader is referred to the Web version of this article.)
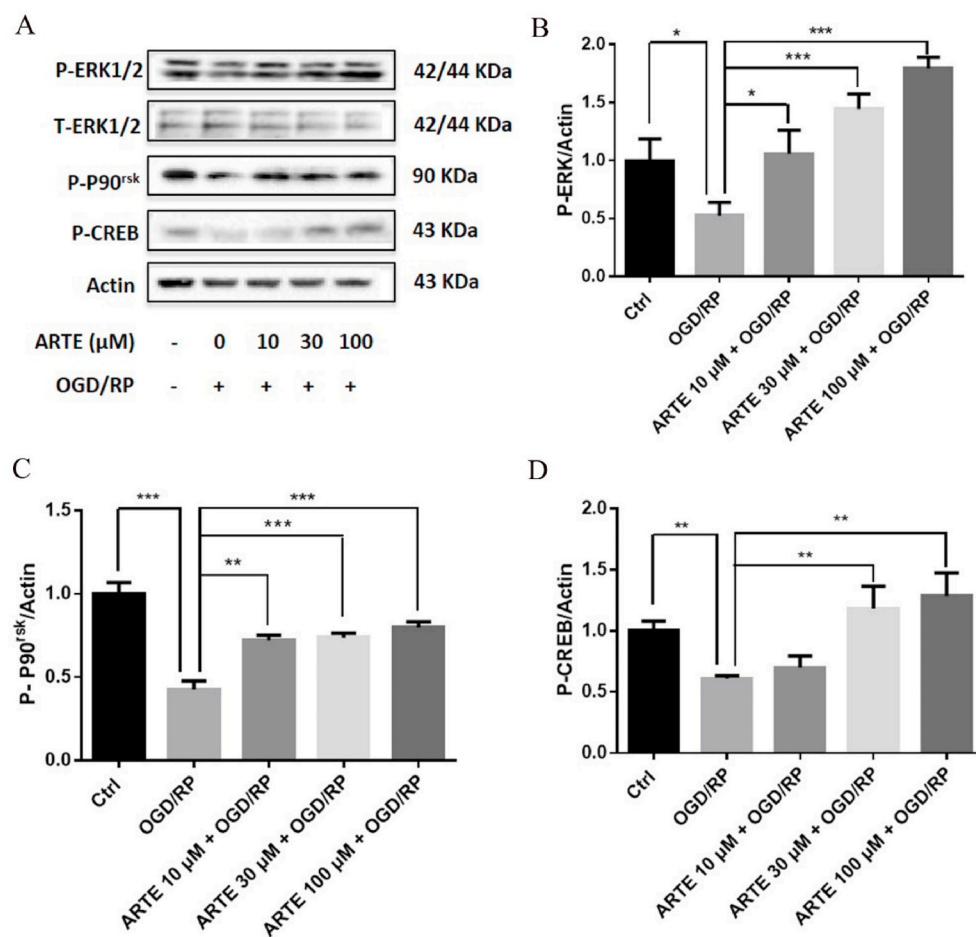
**Fig. 10.** Artemether stimulated the phosphorylation of Erk1/2-P90rsk-CREB in PC12 cells exposed to OGD/RP conditions. PC12 cells were pre-treated with varying concentrations of artemether or 0.1% DMSO (vehicle control) for 2 h and then incubated with or without OGD conditions for 4 h followed by 20 h of reperfusion. (A) Measurement of p-ERK1/2 (p-ERK), total ERK1/2 (T-ERK), P–P90rsk and P-CREB by western blotting. (B, C, D) Quantification of p-ERK and P–P90rsk and P-CREB levels. Three independent experiments were performed in triplicate. *p < 0.05, **p < 0.01, ***p < 0.001 were considered significantly different.

necrotic cell death and this effect was also blocked upon inhibition of ERK1/2 with PD98059 (Fig. 12C). Moreover, artemether (10 μM) reduced intracellular ROS levels, reversed mitochondrial membrane potential ($\triangle\psi m$) and decreased cell apoptosis and these effects were blocked upon inhibition of ERK1/2 with PD98059 (Fig. 12D–I). Assessment of the involvement of Erk1/2-P90rsk-CREB signaling pathway, revealed that similarly to the PC12 cell model, artemether pre-treatment also induced a significant increase in the phosphorylation of ERK1/2, P90rsk and CREB in primary cultured cortical neurons, and these effects were blocked upon inhibition of ERK1/2 with PD98059 (Fig. 12J-M).

### 4. Discussion

This work describes for the first time, the neuroprotective effect of artemether, a derivative of artemisinin, on ischemic stroke. Stroke is an age-related disease and the second most common cause of death [51, 52]. A complex series of biochemical and molecular mechanisms that include excitotoxity, calcium overload, oxidative stress, inflammation and apoptosis are involved in cerebral ischemia-induced impairment, resulting in fatal neuronal death [53]. So far, all therapies, except anti-thrombolytics and hypothermia approaches, have failed to significantly reduce neuronal injury, neurological deficits, and mortality rates following cerebral ischemia, suggesting that the development of novel therapies against stroke is urgently needed. Oxidative stress is one of the most important factors that contribute to ischemic injury. Reactive aldehydes generated from oxidized lipids, such as malondialdehyde (MDA), have been detected in almost all tissues that are subjected to ischemia [54]. Several studies have shown that artemisinin confers

neuroprotection through the resistance to oxidative stress induced by hydrogen peroxide ($H_2O_2$), sodium nitroprusside (SNP), β-amyloid (Aβ) and glutamate [33,55–57]; and artemether (one of artemisinin derivatives) has been reported to be a potential therapeutic agent against AD [32]. However, there are no reports of artemether related to ischemic stroke. Hence, this work aimed to assess the protective effect of artemether in a MCAO stroke animal model and in an OGD/RP cellular model, which have been widely used for studying cerebral ischemia [58, 59]. The establishment of the MCAO experimental animal model required the animals to remain deeply anesthetized for a long period of time. Pentobarbital was the anesthetic of choice has previously described in other studies reporting the use of the same experimental animal model [60–62].Despite being reported to reduce blood pressure (BP), thereby increasing the tolerance to an ischemic insult, this effect is highly dependent of the route of administration being less pronounced with IP administration rather than IV administration [63]. Pentobarbital has also been reported to have a hypothermic effect [64], therefore its administration was performed slowly and a heating pad was used to maintain the body temperature at $37 \pm 0.5\,^{\circ}$C throughout the procedure.

Our results showed that artemether administration to MCAO animal model resulted in a substantial functional recovery, related to the reduction of the brain infarction volume and water content, reduced oxidative stress levels and cell apoptosis, and promotion of cell proliferation. Recently, the role of mitochondria has attracted much attention with regards to cerebral ischemic injury [65–67]. During ischemia, hypoxia depletes intracellular ATP, inactivates oxidative phosphorylation and leads to a compensatory transformation of anaerobic metabolism [68]. Re-introduction of oxygen by reperfusion significantly increases the production of destructive reactive oxygen species
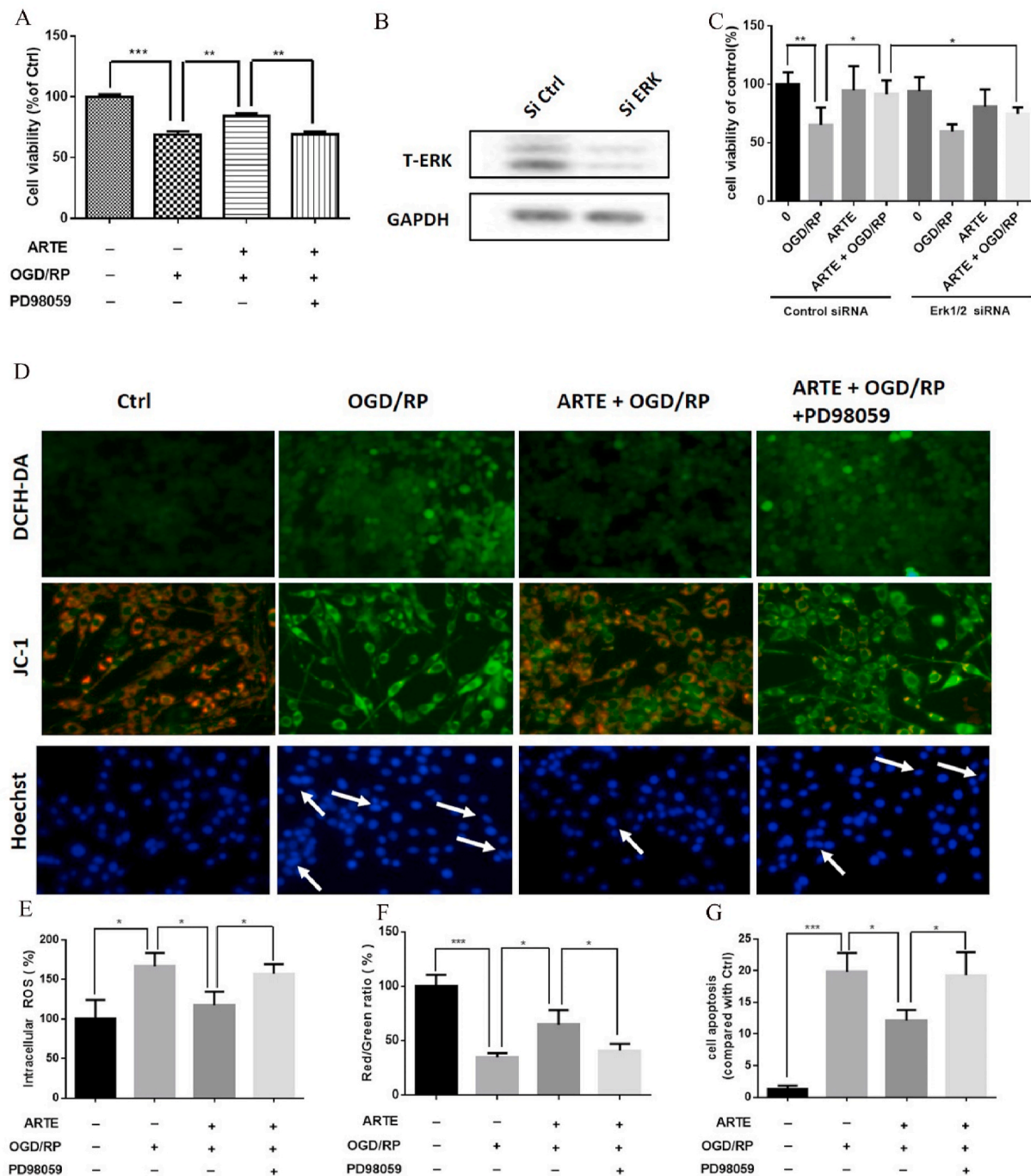
**Fig. 11.** The effect of artemether was blocked by ERK1/2 inhibition or silencing. (A) PC12 cells were pretreated with 25 μM PD98059 (ERK1/2 inhibitor) for 40 min, followed by incubation with artemether 30 μM or 0.1% DMSO (vehicle control) for 2 h and then incubated with or without OGD conditions for 4 h followed by 20 h of reperfusion. Cell viability was measured by MTT assay. (B) Cells were transfected with si-CTRL or si-ERK1/2 and the knock-down efficiency of Erk1/2 was assessed by western blotting. (C) Transfected cells followed were treated with 30 μM artemether or 0.1% DMSO (vehicle control) for 2 h and then incubated with or without OGD conditions for 4 h followed by 20 h of reperfusion. Cell viability was measured by MTT assay. (D) Representative images of ROS, mitochondrial membrane potential and apoptosis on cells pretreated with 25 μM PD98059 (ERK1/2 inhibitor) for 40 min, artemether 30 μM or 0.1% DMSO (vehicle control) for 2 h and incubation with or without OGD conditions for 4 h followed by 20 h of reperfusion. (E, F, G) Quantification of ROS, mitochondrial membrane potential and cell apoptosis. Three independent experiments were performed in triplicate. *p < 0.05, **p < 0.01***p < 0.001 were considered significantly different.

superoxide and hydrogen peroxide from mitochondria [67,69] damaging cellular lipids, proteins and DNA [70]. This leads to the destruction of mitochondrial ATP supply inducing the opening of mitochondrial permeability transition pore, thereby inducing cell death [71,72]. Therefore mitochondrial oxidative damage is a major contributor for ischemic stroke injury. In line with these evidence, our results showed that exposure of cells to OGD/RP conditions caused the collapse

of mitochondrial membrane potential, increased ROS levels and up-regulated Bax/Bcl2 ratio, an indicator of cellular apoptosis. Artemether pretreatment significantly suppressed these changes. Similarly, it also induced a significant change of MDA levels and SOD activity in both *in vitro* and *in vivo* models, suggesting that artemether's antioxidant activity may be involved in its neuroprotective effect on stroke. These results are consistent with our previous studies reporting the antioxidant
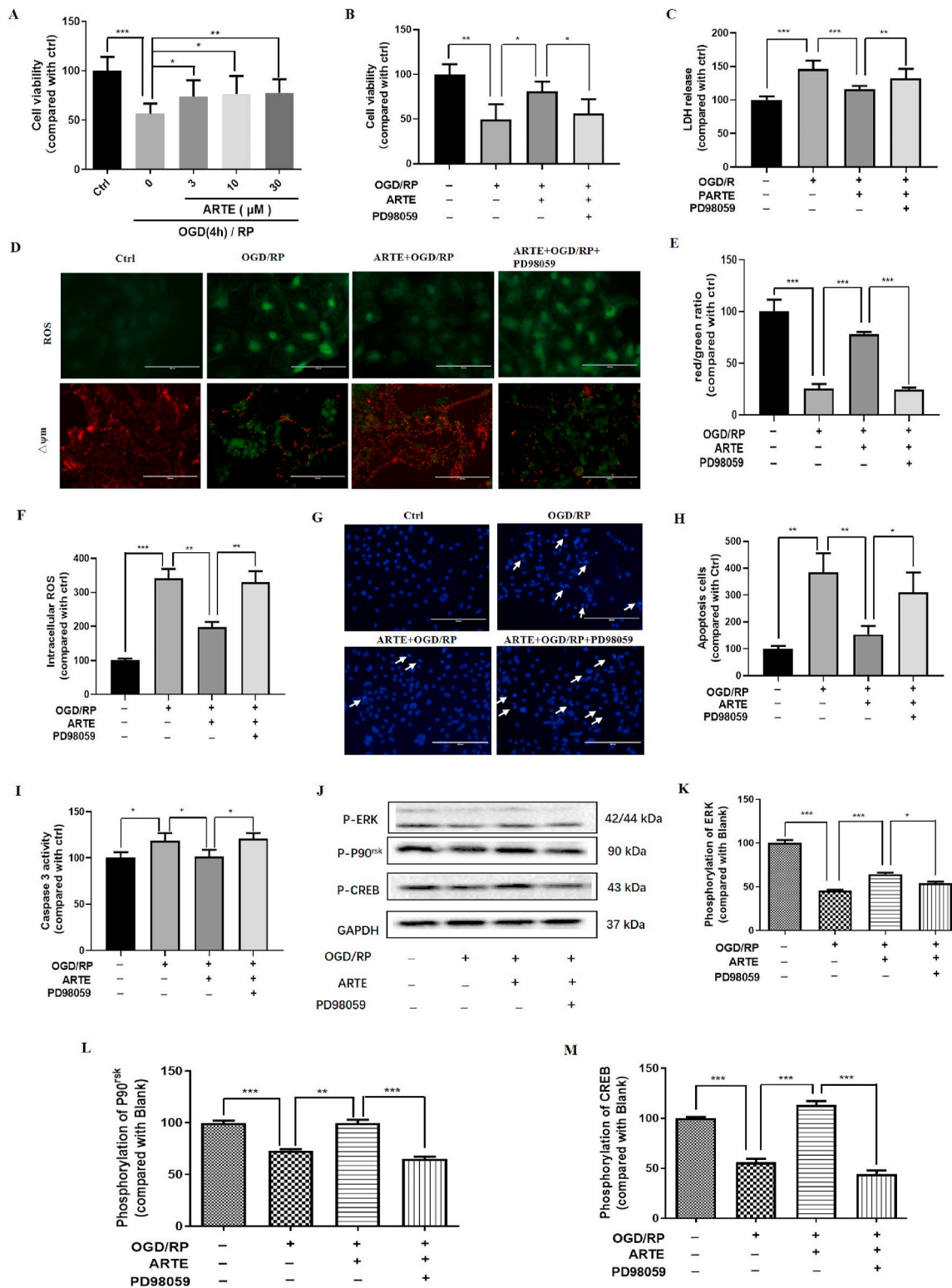
**Fig. 12.** Artemether conferred neuroprotection against OGD/RP-induced cell injury in primary cultured cortical neurons. Primary cultured cortical neurons were prepared and grown according to the commonly used protocols in our laboratory. (A) Cells were pre-treated with varying concentrations of artemether (3–30 μM) or 0.1% DMSO (vehicle control) for 2 h and then incubated with or without OGD conditions for 4 h followed by 20 h of reperfusion. Cell viability was measured by MTT assay. Cells were pre-treated with 20 μM PD98059 (ERK inhibitor) for 30 min before pretreatment with 10 μM artemether or 0.1% DMSO (vehicle control) for 2 h, and then incubated with or without OGD conditions for 4 h followed by 20 h of reperfusion. Cell viability and LDH release were measured by MTT (B) and LDH assays (C). (D) ROS and mitochondrial membrane potential detected by DCFH-DA and JC-1 dye, respectively. (E, F) Quantification of ROS and mitochondrial membrane potential. (G, H) Representative images of apoptosis detected by Hoechst 33,342 and quantification of cell apoptosis. (I) Measurement of Caspase 3 activity. (J) The phosphorylation of ERK, P90rsk and CREB was detected by western blotting. (K, L, M) Quantification of western blotting results. Experiments were performed in triplicate. *p < 0.05, **p < 0.01, ***p < 0.001 were considered significantly different.
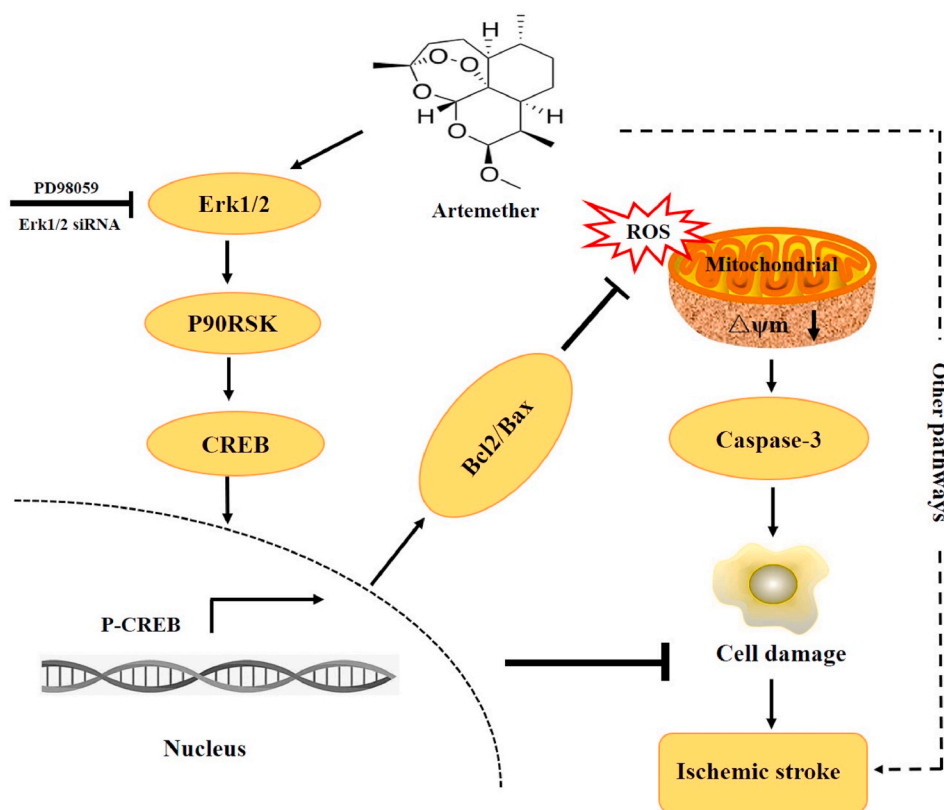
**Fig. 13.** A schematic diagram of artemether confers neuroprotection on cerebral ischemic injury. Artemether stimulated ERK1/2 phosphorylation in PC12 cells, primary cultured cortical neurons and MCAO mouse model, which results in activation of CREB/Bcl-2 pathway and inhibition of apoptosis pathway. All these findings indicate the potential application of artemether in the prevention and treatment of ischemic stroke.

activity of artemether in Aβ-induced injury model and the antioxidant activity of artemisinin [8,9,32,42,43].

Assessment of the involved signaling pathways revealed that ERK1/2 signaling correlated with the neuroprotective effect of artemether in MCAO animal and OGD/RP cellular models through activation of Erk1/2/-P90rsk-CREB signaling cascade. ERK1/2, one of the most extensively studied mitogen-activated protein kinases (MAPK) family members, is involved in the regulation of several cellular processes such as neuronal plasticity, migration and cell survival [73,74]. Evidence also suggest it has a key role in mediating oxidative stress-induced apoptosis [75,76]. Moreover, up-regulation of ERK1/2 signaling activity is associated to a neuroprotective effect in *in vivo* and *in vitro* ischemia stroke models [48,49]. Our results suggest that activation of Erk1/2/-P90rsk-CREB pathway plays a critical role in artemether mediated neuroprotective effect against cerebral ischemic injury. Upon inhibition of ERK1/2, artemether's protective effect against neurological deficits, brain infarction volumes, cell viability, intracellular ROS, mitochondrial membrane potential and cell apoptosis was significantly reduced (Fig. 11).

Artemisinin and its analogues (arts) are used as first-line anti-malarials having also anti-cancer properties. They kill malaria parasites and cancer cells by releasing free radicals which damage the mitochondria and cause apoptosis [77,78]. Arts also target the translationally controlled tumor protein (TCTP) promoting its downregulation and cell apoptosis [79–81]. These reports look contradictory to our present findings describing artemether's neuroprotective effect on stroke. However, our findings were verified in different cellular and animal models with multiple standard evaluation methods. Moreover, the present findings are consistent with our several previous reports describing the protective effect of arts on different neuronal cells against other insults including $H_2O_2$, SNP, corticosterone and β-amyloid [8,33,55]. Importantly, our findings are also supported by studies from other groups in the field. For example, it was reported that artemisinin inhibited glutamate-induced apoptosis in hippocampal neuronal HT-22 cells [57]. Artemisinin also effectively inhibited neuronal apoptosis and improved cognition and memory via regulating histone acetylation and JNK/ERK1/2 signaling [82]. In a different study, artemisinin attenuated doxorubicin-induced cardiotoxicity and hepatotoxicity in rats [83]. Artemisinins treatment also promoted the decrease of the number of TUNEL positive cells in myocardial tissue section [84].

Why arts kill malaria parasites/cancer cells while protecting neuronal cells from different insults is not clear at present but possible in several ways. First, arts usually need high concentrations to kill cancer cells while lower concentrations are used for neuronal protection [85]. Second, the mechanisms in anti-malaria/anti-cancer effect of arts may be different from the ones involved in their neuroprotective effect. In the case of anti-malaria/cancer, arts release free radicals and damage the mitochondria, while for neuronal protection arts reduce the accumulation of ROS, reverse the reduction of mitochondria membrane potential and inhibit apoptosis via activation of ERK, AMPK and P38 [9,34,86]. Third, different artemisinin analogues also have different effects. Some arts are more toxic while others are more protective. For example, artemisinin and artemether are more protective while dihydroartemisinin and artesunate are more toxic and used more often in anti-cancer studies [87,88]. Finally, the effect of arts may be different in different cell types. Arts are more toxic for cancer cells and have a low toxicity on normal cells. These phenomena are also seen in other active components of Chinese traditional medicine such as aloe-emodin [89], astragaloside IV (AS-IV) [90] and berberine [91]. Nevertheless, more studies are necessary to fully uncover the different mechanisms underlying the anti-malaria/cancer and neuronal protection of arts in the future.

In conclusion, our study suggests that artemether has a neuroprotective effect against cerebral ischemic injury via activation of Erk1/

2/-P90rsk-CREB pathway (Fig. 13). Obtained results support the potential use of artemether in the development of more effective therapeutic approaches against ischemic stroke.

## Declaration of competing interest

We declare that we have no financial and personal relationships with other people or organizations that can inappropriately influence our work, there is no professional or other personal interest of any nature or kind in any product, service and/or company that could be construed as influencing the position presented in, or the review of the manuscript entitled "Artemether confers neuroprotection on cerebral ischemic injury through stimulation of the Erk1/2-P90rsk-CREB signaling pathway".

## Acknowledgments

## References

[1] E.S. Donkor, Stroke in the Century: A Snapshot of the Burden, Epidemiology, and Quality of Life. *Stroke Research and Treatment* **2018**, 2018.

[2] G. Yang, et al., Rapid health transition in China, 1990–2010: findings from the global burden of disease study 2010, The lancet 381 (2013) 1987–2015.

[3] R.H. Lee, et al., Cerebral ischemia and neuroregeneration, Neural regeneration research 13 (2018) 373.

[4] J.M. Wardlaw, et al., Recombinant tissue plasminogen activator for acute ischaemic stroke: an updated systematic review and meta-analysis, Lancet 379 (2012) 2364–2372.

[5] X. Gong, N.J. Sucher, Stroke therapy in traditional Chinese medicine (TCM): prospects for drug discovery and development, Trends Pharmacol. Sci. 20 (1999) 191–196.

[6] T. Peng, F. Mohd, P. Lazarovici, L. Chen, W. Zheng, Anti-inflammatory effects of traditional Chinese medicines on preclinical in vivo models of brain ischemia-reperfusion-injury: prospects for neuroprotective drug discovery and therapy, Front. Pharmacol. 10 (2019) 204.

[7] A.M. Dondorp, et al., Artemisinin resistance in Plasmodium falciparum malaria, N. Engl. J. Med. 361 (2009) 455–467.

[8] W. Zheng, et al., Artemisinin conferred ERK mediated neuroprotection to PC12 cells and cortical neurons exposed to sodium nitroprusside-induced oxidative insult, Free Radic. Biol. Med. 97 (2016) 158–167.

[9] C.-M. Chong, W. Zheng, Artemisinin protects human retinal pigment epithelial cells from hydrogen peroxide-induced oxidative damage through activation of ERK/CREB signaling, Redox biology 9 (2016) 50–56.

[10] L. Cui, X.-z. Su, Discovery, mechanisms of action and combination therapy of artemisinin, Expert Rev. Anti-infect. Ther. 7 (2009) 999–1013.

[11] L.C. Okell, et al., Contrasting benefits of different artemisinin combination therapies as first-line malaria treatments using model-based cost-effectiveness analysis, Nat. Commun. 5 (2014) 5606.

[12] A.G. Blazquez, et al., Novel artemisinin derivatives with potential usefulness against liver/colon cancer and viral hepatitis, Bioorg. Med. Chem. 21 (2013) 4432–4441.

[13] A. Das, Anticancer effect of antimalarial artemisinin compounds, Ann. Med. Health Sci. Res. 5 (2015) 93–102.

[14] S. Zhang, et al., Dihydroartemisinin induces apoptosis in human gastric cancer cell line BGC-823 through activation of JNK1/2 and p38 MAPK signaling pathways, Journal of Receptors and Signal Transduction 37 (2017) 174–180.

[15] C. Cheng, et al., Anti-malarial drug artesunate attenuates experimental allergic asthma via inhibition of the phosphoinositide 3-kinase/Akt pathway, PloS One 6 (2011), e20932.

[16] U.P. Okorji, R. Velagapudi, A. El-Bakoush, B.L. Fiebich, O.A. Olajide, Antimalarial drug artemether inhibits neuroinflammation in BV2 microglia through Nrf2-dependent mechanisms, Mol. Neurobiol. 53 (2016) 6426–6443.

[17] T. Efferth, et al., The antiviral activities of artemisinin and artesunate, Clin. Infect. Dis. 47 (2008) 804–811.

[18] C.S.N. Loo, N.S.K. Lam, D. Yu, X.-z. Su, F. Lu, Artemisinin and its derivatives in treating protozoan infections beyond malaria, Pharmacol. Res. 117 (2017) 192–217.

[19] B. Medhi, S. Patyar, R.S. Rao, P.B. Ds, A. Prakash, Pharmacokinetic and toxicological profile of artemisinin compounds: an update, Pharmacology 84 (2009) 323–332.

[20] H. Lu, B. Wang, N. Cui, Y. Zhang, Artesunate suppresses oxidative and inflammatory processes by activating Nrf2 and ROS-dependent p38 MAPK and protects against cerebral ischemia-reperfusion injury, Mol. Med. Rep. 17 (2018) 6639–6646.

[21] D.-x. Yang, et al., Dihydroartemisinin alleviates oxidative stress in bleomycin-induced pulmonary fibrosis, Life Sci. 205 (2018) 176–183.

[22] M. Miloso, A. Scuteri, D. Foudah, G. Tredici, MAPKs as mediators of cell fate determination: an approach to neurodegenerative diseases, Curr. Med. Chem. 15 (2008) 538–548.

[23] M.A. López-Morales, et al., Molecular mechanisms underlying the neuroprotective role of atrial natriuretic peptide in experimental acute ischemic stroke, Mol. Cell. Endocrinol. 472 (2018) 1–9.

[24] T. Jover-Mengual, et al., Molecular mechanisms mediating the neuroprotective role of the selective estrogen receptor modulator, bazedoxifene, in acute ischemic stroke: a comparative study with 17β-estradiol, J. Steroid Biochem. Mol. Biol. 171 (2017) 296–304.

[25] P. Deb, S. Sharma, K. Hassan, Pathophysiologic mechanisms of acute ischemic stroke: an overview with emphasis on therapeutic significance beyond thrombolysis, Pathophysiology 17 (2010) 197–218.

[26] S. Manzanero, T. Santro, T.V. Arumugam, Neuronal oxidative stress in acute ischemic stroke: sources and contribution to cell injury, Neurochem. Int. 62 (2013) 712–718.

[27] R. Scherz-Shouval, Z.R.O.S. Elazar, Mitochondria and the regulation of autophagy, Trends Cell Biol. 17 (2007) 422–427.

[28] Y. Higuchi, Chromosomal DNA fragmentation in apoptosis and necrosis induced by oxidative stress, Biochem. Pharmacol. 66 (2003) 1527–1535.

[29] Y. Gilgun-Sherki, Z. Rosenbaum, E. Melamed, D. Offen, Antioxidant therapy in acute central nervous system injury: current state, Pharmacol. Rev. 54 (2002) 271–284.

[30] S.E. Lakhan, A. Kirchgessner, M. Hofer, Inflammatory mechanisms in ischemic stroke: therapeutic approaches, J. Transl. Med. 7 (2009) 97.

[31] R. Rodrigo, et al., Oxidative stress and pathophysiology of ischemic stroke: novel therapeutic opportunities, CNS Neurol. Disord. - Drug Targets 12 (2013) 698–714.

[32] S. Li, X. Zhao, P. Lazarovici, W. Zheng, Artemether Activation of AMPK/GSK3beta (ser9)/Nrf2 Signaling Confers Neuroprotection towards Beta-Amyloid-Induced Neurotoxicity in 3xTg Alzheimer's Mouse Model, 2019, 1862437, 2019.

[33] Z. Zeng, J. Xu, W. Zheng, Artemisinin protects PC12 cells against beta-amyloid-induced apoptosis through activation of the ERK1/2 signaling pathway, Redox Biol 12 (2017) 625–633.

[34] S.L. Xia Zhao, Uma Gaur, Artemisinin improved neuronal functions in alzheimer's disease animal model 3xtg mice and neuronal cells via stimulating the ERK/CREB signaling pathway, Aging Dis. 2311 (4) (2020 Jul) 801–819.

[35] J. Herz, et al., Exacerbation of ischemic brain injury in hypercholesterolemic mice is associated with pronounced changes in peripheral and cerebral immune responses, Neurobiol. Dis. 62 (2014) 456–468.

[36] E.Z. Longa, P.R. Weinstein, S. Carlson, R. Cummins, Reversible middle cerebral artery occlusion without craniectomy in rats, Stroke 20 (1989) 84–91.

[37] L. Liu, et al., Artemisinin protects motoneurons against axotomy-induced apoptosis through activation of the PKA-Akt signaling pathway and promotes neural stem/progenitor cells differentiation into NeuN(+) neurons, Pharmacol. Res. 159 (2020), 105049.

[38] A. Tjølsen, J.H. Rosland, O.G. Berge, K. Hole, The increasing-temperature hot-plate test: an improved test of nociception in mice and rats, J. Pharmacol. Methods 25 (1991) 241–250.

[39] S. Li, X. Zhao, P. Lazarovici, W. Zheng, Artemether Activation of AMPK/GSK3β (ser9)/Nrf2 Signaling Confers Neuroprotection towards β-Amyloid-Induced Neurotoxicity in 3xTg Alzheimer's Mouse Model, 2019, 1862437, 2019.

[40] S. Hatashita, J.T. Hoff, S.M. Salamat, Ischemic brain edema and the osmotic gradient between blood and brain, J. Cerebr. Blood Flow Metabol. 8 (1988) 552–559.

[41] C. Yang, X. Zhang, H. Fan, Y. Liu, Curcumin upregulates transcription factor Nrf2, HO-1 expression and protects rat brains against focal ischemia, Brain Res. 1282 (2009) 133–141.

[42] X. Zhao, et al., Artemisinin attenuated hydrogen peroxide (H2O2)-induced oxidative injury in SH-SY5Y and hippocampal neurons via the activation of AMPK pathway, Int. J. Mol. Sci. 20 (2019).

[43] S. Li, et al., Artemisinin protects human retinal pigmented epithelial cells against hydrogen peroxide-induced oxidative damage by enhancing the activation of AMP-active protein kinase, Int. J. Biol. Sci. 15 (2019) 2016–2028.

[44] S. Li, et al., Berberine protects human retinal pigment epithelial cells from hydrogen peroxide-induced oxidative damage through activation of AMPK, Int. J. Mol. Sci. 19 (2018).

[45] S. Li, et al., Berberine protects human retinal pigment epithelial cells from hydrogen peroxide-induced oxidative damage through activation of AMPK, Int. J. Mol. Sci. 19 (2018).

[46] J.B. Bederson, et al., Evaluation of 2, 3, 5-triphenyltetrazolium chloride as a stain for detection and quantification of experimental cerebral infarction in rats, Stroke 17 (1986) 1304–1308.

[47] R. Liu, et al., ERK 1/2 activation mediates the neuroprotective effect of BpV (pic) in focal cerebral ischemia–reperfusion injury, Neurochem. Res. 43 (2018) 1424–1438.

[48] T.W. Lai, S. Zhang, Y.T. Wang, Excitotoxicity and stroke: identifying novel targets for neuroprotection, Prog. Neurobiol. 115 (2014) 157–188.

[49] F. Atif, et al., Combination treatment with progesterone and vitamin D hormone is more effective than monotherapy in ischemic stroke: the role of BDNF/TrkB/Erk1/2 signaling in neuroprotection, Neuropharmacology 67 (2013) 78–87.

[50] F. Zhang, J. Chen, Leptin protects hippocampal CA1 neurons against ischemic injury, J. Neurochem. 107 (2008) 578–587.

[51] G.A. Donnan, M. Fisher, M. Macleod, S.M. Davis, Stroke. *Lancet* 371 (2008) 1612–1623.

[52] E.C. Jauch, et al., Part 11: adult stroke: 2010 American heart association guidelines for cardiopulmonary resuscitation and emergency cardiovascular care, Circulation 122 (2010) S818–S828.

[53] H.K. Eltzschig, T. Eckle, Ischemia and reperfusion—from mechanism to translation, Nat. Med. 17 (2011) 1391.

[54] L. He, et al., Alpha lipoic acid protects heart against myocardial ischemia-reperfusion injury through a mechanism involving aldehyde dehydrogenase 2 activation, Eur. J. Pharmacol. 678 (2012) 32–38.

[55] C.M. Chong, W. Zheng, Artemisinin protects human retinal pigment epithelial cells from hydrogen peroxide-induced oxidative damage through activation of ERK/CREB signaling, Redox Biol 9 (2016) 50–56.

[56] W. Zheng, et al., Artemisinin conferred ERK mediated neuroprotection to PC12 cells and cortical neurons exposed to sodium nitroprusside-induced oxidative insult, Free Radical Biol. Med. 97 (2016) 158–167.

[57] S.P. Lin, W. Li, A. Winters, R. Liu, S.H. Yang, Artemisinin prevents glutamate-induced neuronal cell death via akt pathway activation, Front. Cell. Neurosci. 12 (2018) 108.

[58] X. Zhang, et al., Cerebral ischemia-reperfusion-induced autophagy protects against neuronal injury by mitochondrial clearance, Autophagy 9 (2013) 1321–1333.

[59] Z. Shen, et al., PARK2-dependent mitophagy induced by acidic postconditioning protects against focal cerebral ischemia and extends the reperfusion window, Autophagy 13 (2017) 473–485.

[60] X. Bu, et al., Proteomic analysis of cPKCβII-interacting proteins involved in HPC-induced neuroprotection against cerebral ischemia of mice, J. Neurochem. 117 (2011) 346–356.

[61] L. Shu, et al., Inhibition of neuron-specific CREB dephosphorylation is involved in propofol and ketamine-induced neuroprotection against cerebral ischemic injuries of mice, Neurochem. Res. 37 (2012) 49–58.

[62] L. Wang, H. Zhao, Z.-z. Zhai, L.-x. Qu, Protective effect and mechanism of ginsenoside Rg1 in cerebral ischaemia-reperfusion injury in mice, Biomed. Pharmacother. 99 (2018) 876–882.

[63] P.A. Lester, R.M. Moore, K.A. Shuster, D.D. Myers, Anesthesia and analgesia, in: *The laboratory Rabbit, guinea Pig, Hamster, and Other Rodents* 33-56, Elsevier, 2012.

[64] P.L. Hoffman, B. Tabakoff, G. Szabo, P.D. Suzdak, S.M. Paul, Effect of an imidazobenzodiazepine, Ro15-4513, on the incoordination and hypothermia produced by ethanol and pentobarbital, Life Sci. 41 (1987) 611–620.

[65] A.J. Dare, et al., Protection against renal ischemia–reperfusion injury in vivo by the mitochondria targeted antioxidant MitoQ, Redox biology 5 (2015) 163–168.

[66] S. Li, et al., Baicalin attenuates in vivo and in vitro hyperglycemia-exacerbated ischemia/reperfusion injury by regulating mitochondrial function in a manner dependent on AMPK, Eur. J. Pharmacol. 815 (2017) 118–126.

[67] G. Ambrosio, et al., Evidence that mitochondrial respiration is a source of potentially toxic oxygen free radicals in intact rabbit hearts subjected to ischemia and reflow, J. Biol. Chem. 268 (1993) 18532–18541.

[68] P. Devarajan, Update on mechanisms of ischemic acute kidney injury, J. Am. Soc. Nephrol. 17 (2006) 1503–1520.

[69] G. Ambrosio, et al., Oxygen radicals generated at reflow induce peroxidation of membrane lipids in reperfused hearts, J. Clin. Invest. 87 (1991) 2056–2066.

[70] A.-L. Bulteau, et al., Oxidative modification and inactivation of the proteasome during coronary occlusion/reperfusion, J. Biol. Chem. 276 (2001) 30057–30063.

[71] F. Di Lisa, P. Bernardi, Mitochondria and ischemia–reperfusion injury of the heart: fixing a hole, Cardiovasc. Res. 70 (2006) 191–199.

[72] E.J. Lesnefsky, S. Moghaddas, B. Tandler, J. Kerner, C.L. Hoppel, Mitochondrial dysfunction in cardiac disease: ischemia–reperfusion, aging, and heart failure, J. Mol. Cell. Cardiol. 33 (2001) 1065–1089.

[73] M. Drosten, et al., Genetic analysis of Ras signalling pathways in cell proliferation, migration and survival, EMBO J. 29 (2010) 1091–1104.

[74] M.J. Kim, A.W. Dunah, Y.T. Wang, M. Sheng, Differential roles of NR2A-and NR2B-containing NMDA receptors in Ras-ERK signaling and AMPA receptor trafficking, Neuron 46 (2005) 745–760.

[75] Y.J. Lee, et al., Oxidative stress-induced apoptosis is mediated by ERK1/2 phosphorylation, Exp. Cell Res. 291 (2003) 251–266.

[76] Q.H. Tuo, C. Wang, F.X. Yan, D.F. Liao, MAPK pathway mediates the protective effects of onychin on oxidative stress-induced apoptosis in ECV304 endothelial cells, Life Sci. 76 (2004) 487–497.

[77] Q. Xu, et al., Artesunate inhibits growth and induces apoptosis in human osteosarcoma HOS cell line in vitro and in vivo, J. Zhejiang Univ. - Sci. B 12 (2011) 247–255.

[78] A. Robert, J. Cazelles, B. Meunier, Characterization of the alkylation product of heme by the antimalarial drug artemisinin we are grateful to the CNRS for financial support, and to the French ministery of education for a PhD grant to J.C. Dr. Yannick coppel (LCC-CNRS) is gratefully acknowledged for discussions on NMR data, Angew. Chem. 40 (2001) 1954–1957.

[79] Y. Yang, et al., An N-terminal region of translationally controlled tumor protein is required for its antiapoptotic activity, Oncogene 24 (2005) 4778–4788.

[80] Y. Augustin, H.M. Staines, S. Krishna, Artemisinins as a novel anti-cancer therapy: targeting a global cancer pandemic through drug repurposing, Pharmacol. Ther. 216 (2020), 107706.

[81] F. Zhang, et al., Dihydroartemisinin inhibits TCTP-dependent metastasis in gallbladder cancer, J. Exp. Clin. Canc. Res. : CR (Clim. Res.) 36 (2017) 68.

[82] G. Xu, Y.L. Huang, P.L. Li, H.M. Guo, X.P. Han, Neuroprotective effects of artemisinin against isoflurane-induced cognitive impairments and neuronal cell death involve JNK/ERK1/2 signalling and improved hippocampal histone acetylation in neonatal rats, J. Pharm. Pharmacol. 69 (2017) 684–697.

[83] I. Aktaş, Ö. Özmen, H. Tutun, A. Yalçın, A. Türk, Artemisinin attenuates doxorubicin induced cardiotoxicity and hepatotoxicity in rats, Biotech. Histochem. : official publication of the Biological Stain Commission 95 (2020) 121–128.

[84] F. Wang, et al., Artemisinin suppresses myocardial ischemia-reperfusion injury via NLRP3 inflammasome mechanism 474 (2020) 171–180.

[85] X. Zhao, et al., Artemether suppresses cell proliferation and induces apoptosis in diffuse large B cell lymphoma cells, Experimental and therapeutic medicine 14 (2017) 4083–4090.

[86] F. Yan, H. Wang, Y. Gao, J. Xu, W. Zheng, Artemisinin protects retinal neuronal cells against oxidative stress and restores rat retinal physiological function from light exposed damage 8 (2017) 1713–1723.

[87] T. Wang, et al., Dihydroartemisinin suppresses bladder cancer cell invasion and migration by regulating KDM3A and p21, J. Canc. 11 (2020) 1115–1124.

[88] T.K. Våtsveen, et al., Artesunate shows potent anti-tumor activity in B-cell lymphoma, J. Hematol. Oncol. 11 (2018) 23.

[89] X. Dong, Y. Zeng, Aloe-emodin: a review of its pharmacology, toxicity, and pharmacokinetics 34 (2020) 270–281.

[90] J. Zhang, C. Wu, L. Gao, G. Du, X. Qin, Astragaloside IV derived from Astragalus membranaceus: a research review on the pharmacological effects, Adv. Pharmacol. 87 (2020) 89–112.

[91] Y. Wang, Y. Liu, X. Du, H. Ma, J. Yao, The anti-cancer mechanisms of berberine: a review, Canc. Manag. Res. 12 (2020) 695–702.